Wu et al. Mil Med Res 2026
https://doi.org/10.1016/j.mmr.2026.100004

MMR MILITARY MEDICAL RESEARCH

RESEARCH Open Access

USP18 exacerbates myocardial I/R injury by inhibiting Parkin mitophagy through the deubiquitinase PTEN-L

Qing-Qing Wu[1,2†], Yang Xiao[3†], Ying-Ying Hu[1,2], Xiang-Yu Yang[1,2], Xin-Yi Yan[1,2], Ke-Qiong Deng[1,2], Zhi-Li Jin[1,2], Wei Zhang[1,2], Jian-Lei Cao[1,2], Li-Hua Ni[1,2], Yong-Zhen Fan[1,2], Zhi-Bing Lu[1,2*] and Xiao-Rong Hu[1,2*]

Abstract

Background: Mitochondrial quality control is essential for limiting myocardial injury induced by ischemia/reperfusion (I/R), a major contributor to adverse outcomes after reperfusion therapy. This study aimed to determine whether the deubiquitinase ubiquitin-specific protease 18 (USP18) regulates mitophagy during cardiac I/R injury and thereby represents a potential therapeutic target to attenuate myocardial I/R injury.

Methods: Cardiac-specific *USP18* knockout mice were subjected to cardiac I/R injury. To elucidate the role of USP18 in mitophagy regulation and cardiac I/R injury, we performed RNA sequencing, proteomic mass spectrometry, transmission electron microscopy, and mitophagy assays. In parallel, adeno-associated virus serotype 9 (AAV9)-mediated overexpression of USP18, knockdown of *Parkin* and phosphatase and tensin homolog-long (*PTEN-L*), and administration of an anti-PTEN-L neutralizing antibody were used to elucidate the underlying mechanisms. Additionally, serum samples from patients with ST-segment elevation myocardial infarction (STEMI) were collected to assess clinical relevance.

Results: USP18 expression was upregulated in mouse hearts following I/R injury and in ischemic human heart tissue. Cardiac-specific *USP18* deficiency mitigated I/R-induced acute myocardial injury, mitochondrial dysfunction, and adverse cardiac remodeling, whereas USP18 overexpression exacerbated these pathological changes. Mechanistically, USP18 interacted with PTEN-L, which in turn bound to and inhibited the phosphorylation and translocation of Parkin to mitochondria, thereby suppressing mitophagy. *Parkin* knockdown abolished the cardioprotective effects conferred by *USP18* deficiency, whereas *PTEN-L* knockdown reversed the detrimental effect of USP18 overexpression. Moreover, PTEN-L also exerted pathogenic effects via a paracrine mechanism, as neutralizing PTEN-L with an antibody attenuated cardiac I/R injury. Serum PTEN-L levels were elevated in STEMI patients, particularly postintervention.

Conclusions: USP18 impairs mitophagy and exacerbates cardiac I/R injury through a PTEN-L-Parkin axis, involving both intracellular and paracrine mechanisms. Targeting the USP18-PTEN-L pathway may represent a novel therapeutic strategy to alleviate myocardial I/R injury.

Key words Myocardial ischemia/reperfusion (I/R) injury, Ubiquitin-specific protease 18 (USP18), Mitophagy, Phosphatase and tensin homolog-long (PTEN-L), Parkin

Background

Acute myocardial infarction (AMI) results from the sudden blockage of coronary arteries, causing ischemia in the affected area of the myocardium, which often leads to myocardial necrosis [1]. Without timely restoration of coronary perfusion, the development of myocardial scarring occurs, resulting in adverse remodeling of the myocardium; this process can ultimately lead to heart failure [2]. Percutaneous coronary intervention (PCI) is the preferred initial therapy for AMI because of its ability to promptly re-establish coronary perfusion [3]. While restoring blood flow is crucial for preventing ischemic cell death, reperfusion can trigger a spectrum of cell injuries that can be more severe than those induced by ischemia alone [4]. Reperfusion injury, particularly in elderly patients and those with extended ischemia, may counteract the advantages of coronary flow restoration [5]. To date, there is no effective method to prevent ischemia/reperfusion (I/R) injury. A deeper understanding of the mechanisms underlying reperfusion injury could open new treatment strategies for AMI, offering hope for better outcomes.

Maintaining mitochondrial homeostasis is critical for

†Qing-Qing Wu and Yang Xiao contributed equally to this work
*Correspondence: Zhi-Bing Lu, luzhibing@whu.edu.cn; Xiao-Rong Hu, huxrzn@whu.edu.cn
[1]Department of Cardiology, Zhongnan Hospital of Wuhan University, Wuhan 430062, China
Full list of author information is available at the end of the article

Received: 17 June 2025 Accepted: 05 March 2026

preserving cellular physiological functions [5]. During I/R stress, damaged, abnormal, or dysfunctional mitochondria are cleared through a process known as mitochondrial autophagy, also known as mitophagy. Impaired mitophagy and mitochondrial dysfunction are reported to be involved in the initiation and progression of cardiovascular diseases, particularly cardiac I/R injury [6]. By activating mitophagy, empagliflozin confers protection against cardiac microvascular I/R injury [7]. Thus, targeting mitochondrial homeostasis and mitophagy has emerged as a promising therapeutic approach for treating cardiac I/R injury. Among the best-characterized pathways regulating mitophagy is the phosphatase and tensin homolog (PTEN)-induced putative kinase 1 (PINK1)-Parkin axis. Upon mitochondrial depolarization, PINK1 accumulates on the outer mitochondrial membrane and recruits the E3 ubiquitin ligase Parkin, which ubiquitinates multiple mitochondrial surface proteins to trigger mitophagic clearance [8]. In the heart, PINK1-Parkin-mediated mitophagy has been shown to play a protective role in limiting I/R-induced injury [9]. An experimental study in *Parkin*-deficient mice has demonstrated worsened cardiac outcomes following I/R, highlighting the importance of this pathway in myocardial adaptation [10]. Therefore, proper regulation of PINK1-Parkin-dependent mitophagy is critical for mitochondrial quality control and cardiac cell survival under ischemic stress. Recently, Wang *et al*. [11] reported that phosphatase and tensin homolog-long (PTEN-L) is a novel negative regulator of Parkin-mediated mitophagy, exerting its effects through the dephosphorylation of ubiquitin conjugates via its protein phosphatase activity. Thus, targeting the PTEN-L-Parkin-mitophagy pathway may provide promising therapeutic strategies for the treatment of cardiac I/R injury.

Ubiquitination and deubiquitination play pivotal roles in maintaining mitochondrial homeostasis, particularly under pathological conditions such as cardiovascular diseases and cardiac I/R injury [12,13]. Several deubiquitinating enzymes, including ubiquitin-specific protease (USP) 30, USP33, and USP35, have been implicated in the regulation of mitophagy and mitochondrial dynamics in cardiomyocytes [14]. USP33 has been reported to deubiquitinate Parkin and modulate Parkin-mediated mitophagy in neuron-like cells [14,15]. More recently, USP28 was reported to regulate mitochondrial homeostasis and attenuate the progression of diabetic cardiomyopathy [14]. As a prominent member of the deubiquitinase family, USP18 was initially identified for its roles in regulating inflammation, innate antiviral signaling, and cancer progression [16-18]. Recent findings by Ying *et al*. [19] demonstrated that USP18 attenuates angiotensin II-induced pathological cardiac remodeling, indicating a potential role for USP18 in the context of cardiac I/R injury. However, the precise involvement of USP18 in myocardial I/R injury, as well as its underlying regulatory mechanisms, remains largely undefined.

Despite increasing recognition of ubiquitin-dependent mitophagy in protecting the heart against I/R injury, the contribution of deubiquitinating enzymes to this process remains poorly understood. USP18 has been implicated in ubiquitin signaling, yet its role in cardiac I/R injury and mitochondrial quality control is unknown. Therefore, this study aimed to investigate the functional role of USP18 in myocardial I/R injury and to explore the underlying mechanisms involved in USP18-mediated regulation of mitophagy.

Methods

Animals

To establish a cardiac-specific *USP18* knockout mice model (USP18-cKO), $USP18^{flox/flox}$ mice (C57BL/6J; Shanghai Model Organisms, NM-cKO-215042) were bred with α-MHC-MerCreMer mice (C57BL/6J; Jackson Laboratory, stock No. 024992). USP18-cKO ($USP18^{flox/flox}$; α-MHC-MerCreMer) were generated by crossing USP18-cKO mice with α-MHC-MerCreMer transgenic mice. Littermate USP18-cKO mice without Cre served as wild-type (WT) controls. Tamoxifen [20 mg/(kg·d); T-5648, Sigma, MO, USA] was administered intraperitoneally to 6-week-old male mice for 5 consecutive days to induce Cre-mediated recombination.

To induce cardiac-specific USP18 overexpression, male C57BL/6J mice received a single tail vein injection of adeno-associated virus serotype 9 (AAV9)-cardiac troponin T (cTnT)-USP18 or control AAV9-negative control [60–80 μl, $(5.0–6.5)\times10^{13}$ viral genome/ml, Vigene Bioscience, China] under 1.5%–2% isoflurane anesthesia. For the I/R model, each group consisted of 35 mice, with 15 used for acute injury assessment at 24 h and 20 for chronic assessment at 4 weeks; the sham group included 17 mice per group; a total of 108 mice were used. Injections were performed 2 weeks before surgery. For the myocardial knockdown of *PTEN-L* or *Parkin*, male C57BL/6J mice were injected with AAV9-cTnT-shPTEN-L, AAV9-cTnT-shParkin, or control AAV9-ScRNA (Vigene Bioscience, Jinan, China) at the same dose and schedule as described above [20]. To inhibit PTEN-L, mice were administered an anti-PTEN-L antibody (50 μg/mouse, Merck Millipore, USA) on alternate days for 28 d after cardiac I/R surgery. Control animals received vehicle and isotype-matched rat IgG (50 μg/mouse, Sigma, USA). All animal procedures were reviewed and approved by the Animal

Ethics Committee of Zhongnan Hospital, Wuhan University (ZN2023201). To minimize potential bias, all key procedures in our study were performed in a blinded manner.

Neonatal rat cardiomyocyte (NRVM) isolation and treatment

NRVMs were isolated by enzymatic digestion of 1–3-day-old rat hearts, followed by pre-plating to remove nonmyocytes and collection of the enriched cardiomyocyte population following the method described by Liu *et al*. [21]. Adenoviral vectors carrying USP18 (Ad-USP18) and PTEN-L (Ad-PTEN-L) were obtained from Vigene Biosciences (Jinan, China). Truncated PTEN-L was created by deleting the alternatively translated region (ATR) to inhibit its secretion [11]. NRVMs were transduced with adenoviruses [multiplicity of infection (MOI)=100] for gene overexpression or with a control vector (Ad-NC). For knockdown experiments, siRNAs targeting *USP18*, *PTEN-L*, or *Parkin* (RiboBio, Guangzhou, China) or scrambled controls were used. To block mitophagy, the selective dynamin-related protein 1 (Drp1) inhibitor Mdivi-1 was used (50 μmol/L, MedChemExpress, USA). Cells were incubated under hypoxic conditions (95% N_2, 5% CO_2) for 4 h, followed by reoxygenation under normoxia (95% air, 5% CO_2) overnight to induce a hypoxia/reoxygenation (H/R) model. USP18 expression in NRVMs was induced by treatment with tumor necrosis factor-α (TNF-α, 5 ng/ml; Beyotime, China) [22] or high mobility group box 1 (HMGB1, 100 ng/ml; Abcam, USA) [23] for 6 h.

Human samples

Left ventricular (LV) samples were obtained from heart transplant recipients with ischemic heart disease (IHD) and from normal heart donors [24].

Serum samples were collected retrospectively. Thirty AMI patients were recruited from Zhongnan Hospital between January 1, 2025, and June 30, 2025. The diagnostic criteria included 1) creatine kinase-MB isoenzyme (CK-MB) levels at least twice the normal range or a cardiac troponin I (cTnI) concentration >0.1 ng/ml and 2) the presence of new Q waves or ST-segment/T-wave abnormalities on electrocardiography. Patients with thrombolysis in myocardial infarction flow grade 0–2 received immediate revascularization, including percutaneous coronary angioplasty and stent placement. Revascularization was considered successful if thrombolysis in myocardial infarction flow grade 3 flow was achieved without significant residual stenosis. The exclusion criteria included previous myocardial infarction, stent implantation, bypass surgery, cardiomyopathies, myocarditis, acute heart failure, malignancies, inflammatory or autoimmune diseases, and transplant patients. The control subjects were patients with normal coronary angiograms and no diagnosis of coronary artery disease.

All the subjects provided written informed consent before participation. Serum samples from AMI patients were obtained before and after PCI. The study protocol was approved by the Ethics Committee of Zhongnan Hospital (2025058K) and complied with the principles of the Declaration of Helsinki.

Other experimental procedures

Other experimental procedures including mouse model, biochemical analysis, echocardiography, histological analysis, ELISA assessment of inflammatory cytokines, electron microscopy, mitochondrial respiratory complexes, transcriptomic profiling, mitochondrial functional, imaging, and *in vitro* mitophagy analyses, co-immunoprecipitation (Co-IP) and high-performance liquid chromatography-tandem mass spectrometry analysis, ubiquitination assays, luciferase activity analysis, phosphorylation-tag gel electrophoresis, and Western blotting, are described in detail in Additional file 1. Additional file 1: Table S1 lists all the primer sequences used in RT-PCR [5].

Statistical analysis

SPSS 23.3 was used for data analysis. A power analysis with 95% power and α=0.05 indicated that a sample size of at least 5 mice per group was required for function and morphometry analysis and a minimum of 3 mice per group for the molecular analysis [25]. We routinely exceeded the minimal number of mice required for each experiment, as indicated in the figure legends. For multiple group comparisons, one-way ANOVA was used. When the ANOVA indicated significance and variance was homogeneous, the least significant difference (LSD) post hoc test was applied; otherwise, Tamhane's T2 test was used. Comparisons between two groups were performed using an unpaired Student's *t*-test. Specifically, all hypothesis tests were two-tailed to account for potential effects in both directions. All experiments, including *in vivo*, *in vitro*, and imaging studies, were conducted blinded. Statistical significance was defined as $P<0.05$. For clinical data, the Mann-Whitney *U* test and χ^2 test were applied for continuous and categorical clinical variables, respectively, with $P<0.05$ considered significant. Between-variable correlations were assessed by Spearman's test.

Results

USP18 expression is induced by cardiac I/R injury

USP18 expression has been found in various tissues, with

particularly high levels in macrophages and bone marrow-derived dendritic cells. Its levels notably increase following viral or bacterial infections [26]. Gene expression profiles of LV tissues from mice exposed to 24 h I/R were analyzed and compared to those of control mice to identify potential key regulators of cardiac I/R injury. Gene Ontology (GO) analysis revealed a significant enrichment in ubiquitin-mediated protein regulation (Fig. 1a). An in-depth analysis of the ubiquitin-related differentially expressed genes revealed 14 upregulated genes and 2 downregulated genes (Fig. 1b). Notably, the upregulation of USP18 expression was most prominent in I/R hearts. Data from the Human Protein Atlas indicated that USP18 was highly expressed in the liver, testis, breast, and skin, with moderate expression in the heart (Additional file 1: Fig. S1a). To further investigate the involvement of USP18 in cardiac I/R injury, we assessed the protein levels of USP18 in human heart samples obtained from donors and individuals diagnosed with IHD. As anticipated, USP18 expression was upregulated in heart tissue affected by IHD (Fig. 1c, d). Upon reanalysis of the RNA sequencing (RNA-seq) data obtained from end-stage IHD human hearts (GSE203160), we observed increased expression of USP18, as depicted in Additional file 1: Fig. S1b. In murine hearts subjected to I/R injury, USP18 expression progressively increased from 24 h to 4 weeks post-surgery (Fig. 1e; Additional file 1: Fig. S1c). Dual immunofluorescence labeling of USP18 and wheat germ agglutinin revealed minimal baseline expression of USP18, which was significantly elevated in cardiac tissue post-I/R and was predominantly localized within cardiomyocytes (Fig. 1f; Additional file 1: Fig. S1c). The level of USP18 remained unchanged in cardiac fibroblasts, endothelial cells, and macrophages in response to cardiac I/R stress (Additional file 1: Fig. S1c, d). *In vitro* studies also revealed that USP18 expression was significantly upregulated following H/R injury at 6, 12, and 24 h in NRVMs (Fig. 1g) and was predominantly localized in the cytoplasm (Fig. 1h). Collectively, these findings suggest that USP18 expression is induced by cardiac I/R injury.

Another question to be answered was the regulation of USP18 expression during cardiac I/R injury. USP18 expression is strongly induced by type I and III interferons, lipopolysaccharide, and TNF-α [26]. Because inflammation is strongly associated with acute cardiac I/R injury, we explored whether these inflammatory factors mediate the upregulation of USP18 expression during cardiac I/R injury. NRVMs were treated with TNF-α and HMGB1, a key inflammatory mediator during myocardial infarction. The protein level of USP18 sharply increased upon TNF-α and HMGB1 stimulation (Additional file 1: Fig. S1e). Moreover, the increase in USP18 expression was significantly suppressed in H/R-stressed NRVMs by TNF-α or HMGB1 antibodies (Additional file 1: Fig. S1f). Luciferase assays revealed that stimulation with TNF-α and HMGB1 led to a significant increase in USP18 transcription (Additional file 1: Fig. S1g).

USP18 deficiency mitigates mitochondrial dysfunction, acute cardiac I/R injury, and cardiac remodeling *in vivo*

To investigate the role of USP18 in cardiac I/R injury, we established cardiac-specific USP18-cKO mice and confirmed them by Western blotting (Additional file 1: Fig. S2a). Compared with WT control mice, USP18-cKO mice had a diminished infarct size following cardiac I/R injury, despite receiving the same surgical treatment (Fig. 2a). At 4 h post-I/R, the serum levels of cTnT, CK-MB, and lactate dehydrogenase (LDH) were significantly lower in USP18-cKO mice than in control mice, indicating that cardiac injury was mitigated (Additional file 1: Fig. S2b). The loss of USP18 led to decreased overall apoptosis following I/R injury, as indicated by decreased DNA fragmentation and reduced cleaved caspase-3 activity in the LV (Additional file 1: Fig. S2c). USP18 has been shown to influence innate antiviral immunity by shifting tripartite motif-containing protein 31 from the cytoplasm to the mitochondria [18]. These findings suggest a potential impact of USP18 on mitochondrial function. We subsequently assessed mitochondrial morphology and function. USP18-cKO mice exhibited increased mitochondrial DNA content and ameliorated activity of mitochondrial complexes I and II–III (Fig. 2b). USP18-cKO mice showed attenuation of I/R-induced mitochondrial loss and cristae disarray, indicating preserved mitochondrial structure (Fig. 2c). The mitochondrial dysfunction induced by I/R injury was also alleviated by *USP18* knockdown, as evidenced by an increased respiratory oxygen consumption rate (OCR) and elevated basal, ATP-related, and maximal respiration, while no difference in spare respiration (Fig. 2d).

To further investigate the long-term effects of USP18 on cardiac function under physiological conditions and on cardiac remodeling after cardiac I/R injury, we observed the animals over an extended timeline. The cardiac function of USP18-cKO mice at 2, 4, 6, and 12 months was comparable to that of their WT littermates, as shown in Additional file 1: Fig. S2d. Compared with WT mice, USP18-cKO mice displayed less cardiomyocyte enlargement, diminished LV fibrotic remodeling, and a decreased heart weight-to-tibia length ratio (HW/TL) (Fig. 2e; Additional file 1: Fig. S2e). The transcriptional activation of hypertrophic and fibrotic markers, including atrial natriuretic peptide (*ANP*), B-type natriuretic

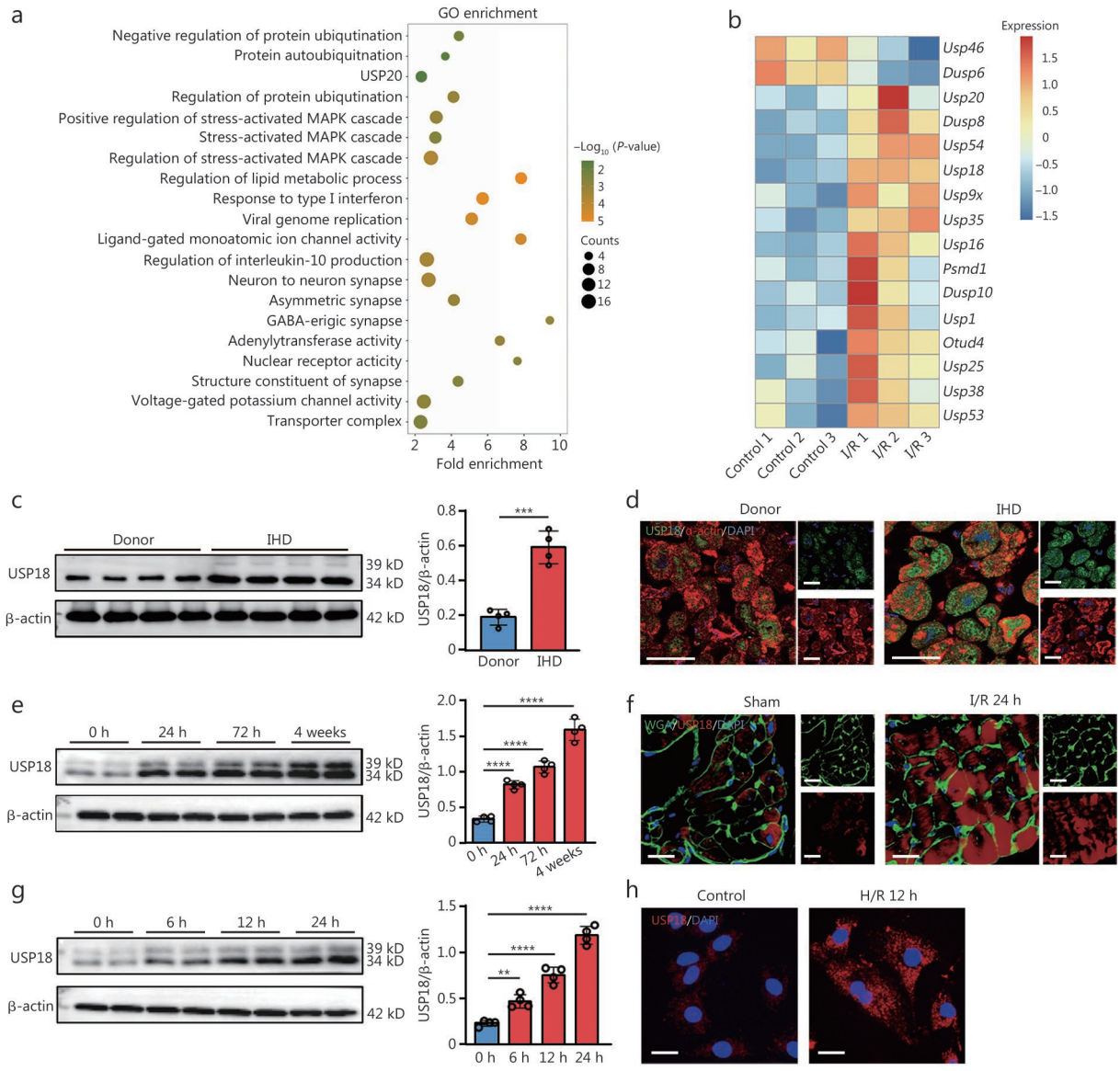

Fig. 1 USP18 expression is induced by cardiac I/R injury.

a Gene Ontology (GO) enrichment analysis of the RNA-seq data in I/R and control hearts at 24 h postsurgery (n=3). **b** Heatmap displaying differentially expressed ubiquitination-associated genes in I/R and control hearts at 24 h postsurgery (n=3). **c** Protein levels of USP18 in donor heart tissue and patients with ischemic heart disease (IHD) (n=4). **d** Immunofluorescence staining of USP18 and α-actin in donor heart tissue and patients with IHD (n=3). Scale bar=35 μm (left) and 50 μm (right). **e** Protein levels of USP18 in heart tissue post-IR (n=4). **f** Immunofluorescence staining of USP18 and WGA in heart tissue 24 h after I/R injury (n=5). Scale bar=50 μm. **g** Protein expression of USP18 in primary neonatal rat cardiomyocytes (NRVMs) after H/R challenge (n=4). **h** Immunofluorescence staining of USP18 in cardiomyocytes after H/R challenge. Scale bar=50 μm. **P<0.01, ***P<0.001, ****P<0.0001. USP18. Ubiquitin-specific protease 18; I/R. Ischemia/reperfusion; WGA. Wheat germ agglutinin; DAPI. 4′,6-diamidino-2-phenylindole; H/R. Hypoxia/reoxygenation; RNA-seq. RNA sequencing; MAPK. Mitogen-activated protein kinase; GABA. γ-aminobutyric acid

peptide (*BNP*), and *collagen I* and *III*, was significantly suppressed in USP18-cKO hearts 4 weeks after I/R injury (Additional file 1: Fig. S2f). USP18-cKO mice showed improved cardiac function and attenuated ventricular dilation following I/R injury, as evidenced by elevated LV ejection fraction and LV fractional shortening, along with decreased left ventricle internal diameter at diastole (LVIDd), left ventricle internal diameter at systole (LVISd), and heart rate (Fig. 2f, g). Overall, the results of the genetic ablation of cardiac USP18 reveal its pathogenic contribution to mitochondrial disruption, acute I/R-induced myocardial damage, and long-term adverse ventricular remodeling in murine hearts.

Pathological effects of cardiac USP18 overexpression on mitochondrial function and after ischemic remodeling

We next investigated whether overexpression of USP18 could exacerbate these pathologies. To test this hypothesis, C57BL mice were administered a single tail vein injection of AAV9-USP18 two weeks before I/R surgery, which resulted in abundant USP18 expression in heart tissue (Additional file 1: Fig. S3a). USP18-overexpressing (OV) mice had a larger infarct area 24 h after cardiac I/R injury (Fig. 3a). Elevated serum levels of cTnI, CK-MB, and LDH were observed in

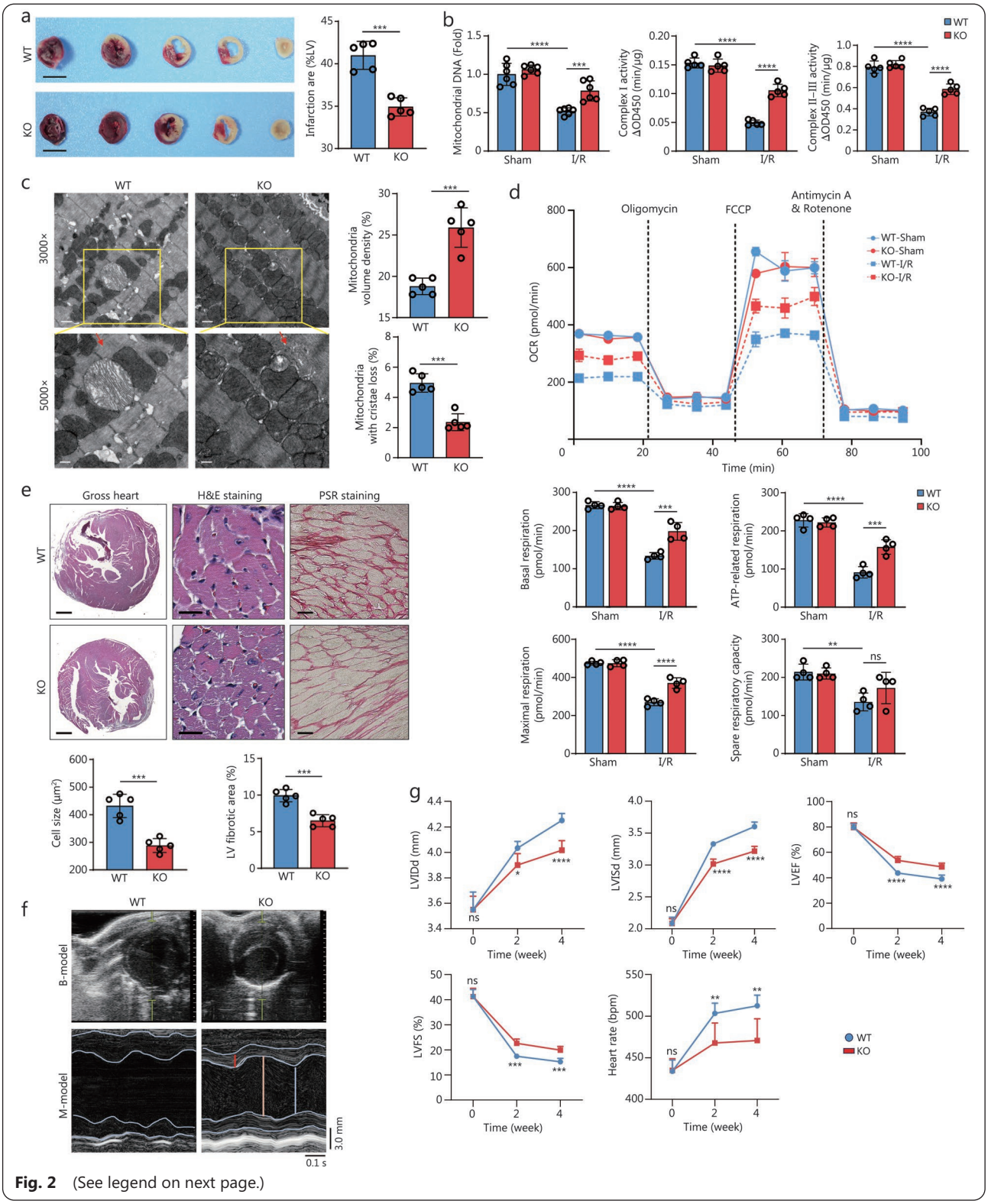

Fig. 2 (See legend on next page.)

(See figure on previous page.)

Fig. 2 ***USP18* deficiency mitigates mitochondrial dysfunction, acute cardiac I/R injury, and cardiac remodeling *in vivo*.** **a** 2,3,5-triphenyltetrazolium chloride (TTC) staining of heart tissue 24 h post-I/R in WT and I/R groups (n=5). Scale bar=0.5 cm. ***P<0.001. **b** Mitochondrial DNA (n=6) and mitochondrial complexes I and II–III activity (n=5) 24 h post-I/R in each group. **P<0.01, ****P<0.0001. **c** Representative electron microscopy images of heart sections 24 h post-I/R; quantitative analysis of the mitochondrial volume density and percent of mitochondria with cristae loss in each group (n=5). Scale bar=10 μm (top) and 6 μm (bottom). Red arrows indicate mitochondria with cristae loss ***P<0.001. **d** Oxygen consumption rate (OCR) and quantitative statistical analysis of basal respiration, ATP-related respiration, maximal respiration, and spare respiratory capacity in mitochondria in the indicated groups (n=4). **P<0.01, ****P<0.0001, ns non-significant. **e** H&E staining, PSR staining, and quantitative statistical analysis of cell size and left ventricle (LV) fibrotic area in WT mice and USP18-cKO mice at 4 weeks after I/R injury (n=5). Scale bar=1 mm (left), 50 μm (middle), and 100 μm (right). **P<0.01. **f** Representative B-mode and M-mode echocardiographic images of LV from WT mice or USP18-cKO mice 4 weeks after I/R injury. **g** Cardiac function of WT mice and USP18-cKO mice after I/R injury at the indicated time points (n=6). *P<0.05, **P<0.01, ***P<0.001, ****P<0.0001 vs. WT, ns non-significant. USP18. Ubiquitin-specific protease 18; I/R. Ischemia/reperfusion; WT. Wild-type; ATP. Adenosine triphosphate; H&E. Hematoxylin and eosin; PSR. Picrosirius red; FCCP. Carbonyl cyanide p-trifluoromethoxyphenylhydrazone; USP18-cKO. Ubiquitin-specific protease 18 conditional knockout; LVIDd. Left ventricle internal diameter at diastole; LVISd. Left ventricle internal diameter at systole; LVEF. Left ventricle ejection fraction; LVFS. Left ventricle fractional shortening

USP18-OV mice 4 h after cardiac I/R (Additional file 1: Fig. S3b). An increased DNA fragment was also observed in USP18-OV hearts following I/R injury (Additional file 1: Fig. S3c). Additionally, overexpression of USP18 in the heart significantly exacerbated mitochondrial dysfunction, as evidenced by decreased mitochondrial density, increased disarrayed cristae, reduced mitochondrial DNA content, and decreased activity of mitochondrial complexes I and II–III in I/R injury mice (Fig. 3b, c). The mitochondrial dysfunction induced by I/R injury was exacerbated by USP18 overexpression, as evidenced by a decreased respiratory OCR and decreased basal, maximal, and spare respiration (Fig. 3d).

Cardiac-specific overexpression of USP18 led to a decline in cardiac function, starting at 6 months of age and becoming particularly pronounced at 12 months (Additional file 1: Fig. S3d). USP18-OV mice displayed pronounced cardiac remodeling 4 weeks after I/R, as evidenced by hypertrophic cardiomyocytes, expanded fibrotic regions, and an elevated HW/TL, in accordance with their acute injury severity (Fig. 3e; Additional file 1: Fig. S3e). Mice with USP18 overexpression exhibited increased mRNA transcription of cardiac hypertrophic and fibrosis markers at 4 weeks after I/R injury (Additional file 1: Fig. S3f). LVEF and LVFS were decreased, while LVIDd, LVISd, and heart rate were aggravated in USP18-OV mice after I/R injury (Fig. 3f, g). Collectively, these findings reveal that the cardiac-specific overexpression of USP18 intensifies mitochondrial dysfunction, acute ischemic injury, and subsequent structural and functional deterioration in post-I/R hearts.

Effects of USP18 on H/R-induced injury to NRVMs

To confirm the role of USP18 *in vitro*, NRVMs were transfected with USP18 siRNA to silence endogenous USP18 expression. Western blotting analysis demonstrated that USP18 expression was downregulated in H/R-treated NRVMs following USP18 siRNA transfection (Additional file 1: Fig. S4a). *USP18* knockdown led to a significant increase in cell viability, decreased LDH release, and reduced cleaved caspase-3 activity, along with diminished formation of DNA fragments in H/R-stimulated NRVMs (Additional file 1: Fig. S4b). Furthermore, *USP18* knockdown in NRVMs mitigated mitochondrial damage induced by H/R stress, as evidenced by longer mitochondrial length and fewer mitochondrial fragments, accompanied by increased mitochondrial DNA content (Fig. 4a, b). The mitochondrial dysfunction induced by H/R stress was also alleviated by *USP18* knockdown, as evidenced by increased OCR and elevated basal and maximal respiration, but no difference in ATP-related and spare respiration (Fig. 4c, d).

Consistent with the *in vivo* findings, in NRVMs transfected with Ad-USP18 to overexpress USP18 (as validated by Western blotting; Additional file 1: Fig. S4c), H/R injury-induced cell injury and death were dramatically exacerbated by USP18 overexpression (Additional file 1: Fig. S4d). H/R injury-induced mitochondrial dysfunction was also exacerbated by USP18 overexpression in NRVMs, as evidenced by shorter mitochondrial length, increased mitochondrial fragmentation, decreased mitochondrial DNA content, and reduced OCR with decreased basal and ATP-related respiration, but no difference in maximal and spare respiration (Fig. 4e-h). Collectively, our findings demonstrate that USP18 exacerbates mitochondrial dysfunction and cardiac I/R injury both *in vivo* and *in vitro*.

USP18 aggravates cardiac I/R injury through regulation of mitochondria and inhibition of mitophagy

To assess the molecular impact of USP18, we conducted RNA-seq analysis of heart samples 24 h after LV tissue

isolation from USP18-cKO-I/R and WT-I/R mice. Metabolic regulation and mitophagy were the most enriched pathways in *USP18*-deficient hearts following I/R, as determined by Kyoto Encyclopedia of Genes and Genomes (KEGG) analysis (Additional file 1: Fig. S5a, b). A heatmap revealed that USP18-cKO significantly regulated the expression of genes involved in mitochondrial activity and metabolic events (Additional file 1: Fig. S5c). Indeed, Gene Set Enrichment Analysis of

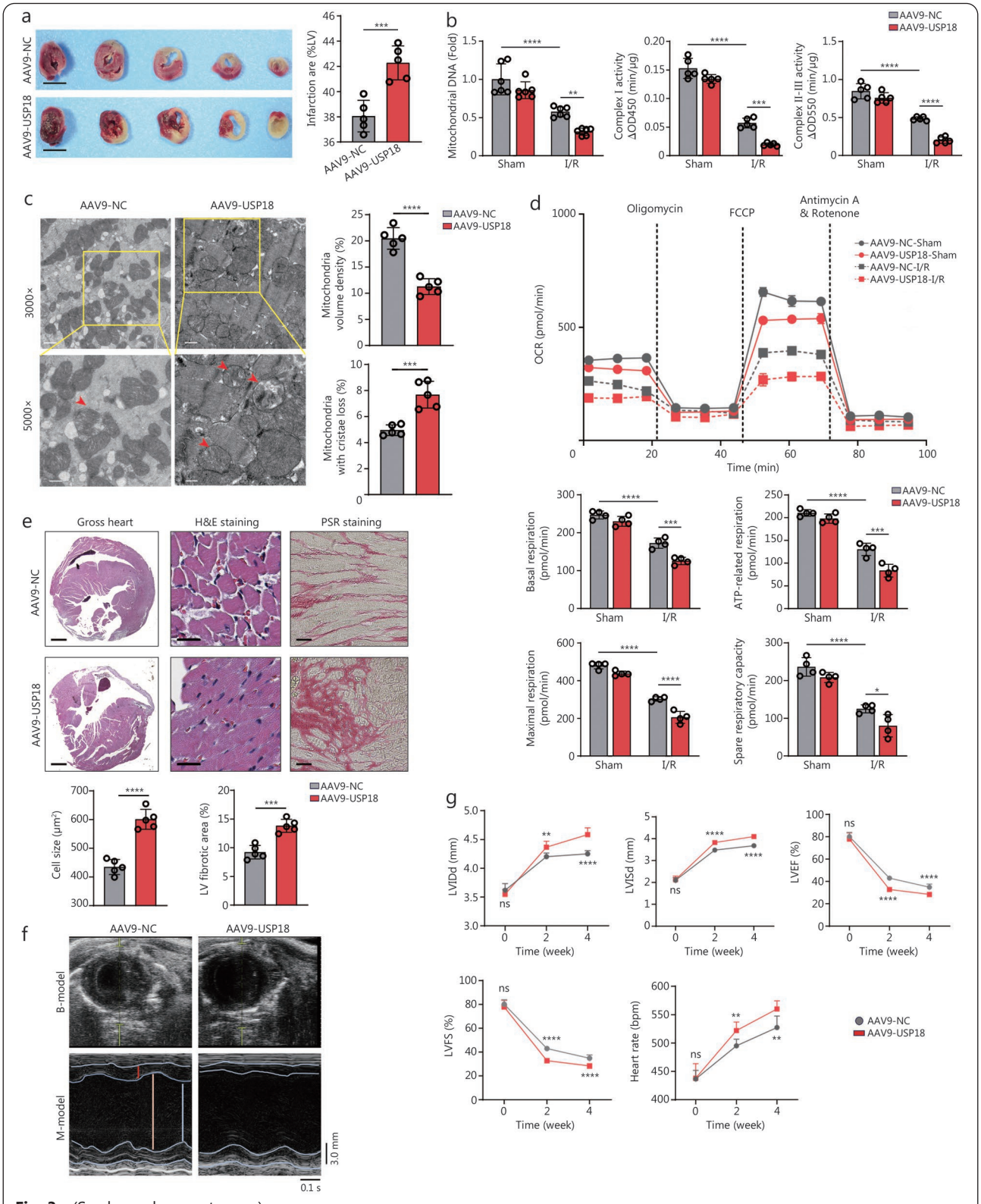

Fig. 3 (See legend on next page.)

(See figure on previous page.)

Fig. 3 Overexpression of USP18 in the heart exacerbates mitochondrial dysfunction, acute cardiac injury, and cardiac remodeling following I/R in mice.

a TTC staining of heart tissue 24 h post-I/R in each group (n=5). Scale bar=0.5 cm. ***P<0.001. **b** Mitochondrial DNA levels (n=6) and mitochondrial complexes I and II–III activity (n=5) 24 h post-I/R in each group. **P<0.01, ***P<0.001, ****P<0.0001. **c** Representative electron microscopy images of heart sections 24 h post-I/R. Quantitative analysis of mitochondrial volume density and the percent of mitochondria with cristae loss in each group (n=5). Scale bar=10 μm (top) and 6 μm (bottom). Red arrows indicate mitochondria with cristae loss. ***P<0.001, ****P<0.0001. **d** Oxygen consumption rate (OCR) and quantitative statistical analysis of basal respiration, ATP-related respiration, maximal respiration, and spare respiratory capacity in mitochondria in the indicated groups (n=4). *P<0.05, ***P<0.001, ****P<0.0001. **e** H&E staining, PSR staining, and quantitative statistical analysis of cell size and left ventricle (LV) fibrotic area in AAV9-USP18-transfected mice at 4 weeks after I/R injury (n=5). Scale bar=1 mm (left), 50 μm (middle), and 100 μm (right). ***P<0.001, ****P<0.0001. **f** Representative B-mode and M-mode echocardiographic images of LV from AAV9-USP18-transfected mice 4 weeks after I/R injury. **g** Cardiac function of AAV9-USP18-transfected mice after I/R injury at the indicated time points (n=6). **P<0.01, ***P<0.001, ****P<0.0001 vs. AAV9-NC, ns non-significant. USP18. Ubiquitin-specific protease 18; I/R. Ischemia/reperfusion; NC. Negative control; AAV9. Adeno-associated virus serotype 9; AAV9-USP18. Adeno-associated virus serotype 9 encoding USP18; TTC. 2,3,5-triphenyltetrazolium chloride; ATP. Adenosine triphosphate; H&E. Hematoxylin and eosin; PSR. picrosirius red; FCCP. Carbonyl cyanide p-trifluoromethoxyphenylhydrazone; LVIDd. Left ventricle internal diameter at diastole; LVISd. Left ventricle internal diameter at systole; LVEF. Left ventricle ejection fraction; LVFS. Left ventricle fractional shortening

the RNA-seq data further confirmed that mitochondrial-related GO pathways were significantly increased by *USP18* deletion in I/R-induced hearts (Additional file 1: Fig. S5d). Both loss-of-function and gain-of-function studies revealed the effect of USP18 on mitochondrial function. Because mitochondrial dysfunction plays a crucial role in mediating pathophysiological processes in cardiac I/R injury and impaired mitophagy accelerates mitochondrial dysfunction and cardiac I/R injury, it is plausible that the effects of USP18 on mitochondrial function may contribute to its role in cardiac I/R injury [6]. Transmission electron microscopy revealed that the impaired mitophagy observed in I/R mice was restored in the hearts of USP18-cKO mice (Fig. 5a). I/R induction also increased the levels of PTEN-induced PINK1, Parkin, P62, and microtubule-associated protein 1 light chain 3-II (LC3II), and the level of ubiquitinated proteins (Ub) in mitochondria (Fig. 5b). During I/R injury, PINK1 and Parkin accumulate on damaged mitochondria in response to cellular stress. This process leads to the isolation of damaged mitochondria from the mitochondrial network and directs them toward autophagic degradation [27]. USP18-cKO mice presented significantly increased protein levels of PINK1, Parkin, Ub, P62, and LC3II in the mitochondria (Fig. 5b). The impairment of mitophagy was exacerbated in USP18-OV mouse hearts (Fig. 5c). USP18-OV reduced the levels of PINK1, Parkin, Ub, P62, and LC3II in mitochondria (Fig. 5d).

We also visualized mitophagy *in vitro* by using a mitophagy dye and a lysosomal dye in NRVMs. This dual-fluorescent probe system indicates the pH changes as mitophagy fluorescence (red) increases in the acidic lysosomal compartment (green). Mitophagic fluorescence was increased in *USP18*-knockdown cardiomyocytes, indicating increased mitophagy flow (Fig. 5e). Conversely, decreased mitophagy signaling was observed in USP18-OV cardiomyocytes, indicating impaired mitophagy flow (Fig. 5f). The protein levels of PINK1, Parkin, Ub, P62, and LC3II in mitochondria were increased in *USP18*-knockdown cardiomyocytes but reduced in USP18-OV cardiomyocytes during I/R injury (Fig. 5g, h). These data suggest that by inhibiting PINK1/Parkin-mediated mitophagy signaling, USP18 may act as a detrimental factor during cardiac I/R injury.

Key markers of mitochondrial fission [p-Drp1 (Ser616)], fusion [mitofusin 2 (MFN2), mitofusin 1 (MFN1)], biogenesis [peroxisome proliferator-activated receptor gamma coactivator-1α (PGC-1α) and mitochondrial transcription factor A (TFAM)], and other mitophage-related proteins [BCL2 interacting protein 3 (BNIP3), and FUN14 domain containing 1 (FUNDC1)] were also assessed. As shown in Additional file 1: Fig. S6a, b, neither genetic deletion nor overexpression of USP18 resulted in significant changes in the levels of these markers, suggesting that USP18 does not substantially affect mitochondrial fission, fusion, or biogenesis in the context of cardiac I/R injury. USP18 increased the expression of apoptosis-associated proteins (Bax, Bcl-2), but this effect was hampered by USP18-cKO (Additional file 1: Fig. S6a, b). These results support the notion that USP18 selectively impairs PINK1/Parkin-mediated mitophagy rather than broadly disrupting mitochondrial quality control mechanisms. *USP18* knockdown significantly reduced mitochondrial reactive oxygen species (ROS) levels following H/R stress. In contrast, USP18 overexpression markedly increased mitochondrial ROS levels under the same conditions (Additional file 1: Fig. S6c, d). Improved mitochondrial clearance likely contributed to reduced ROS

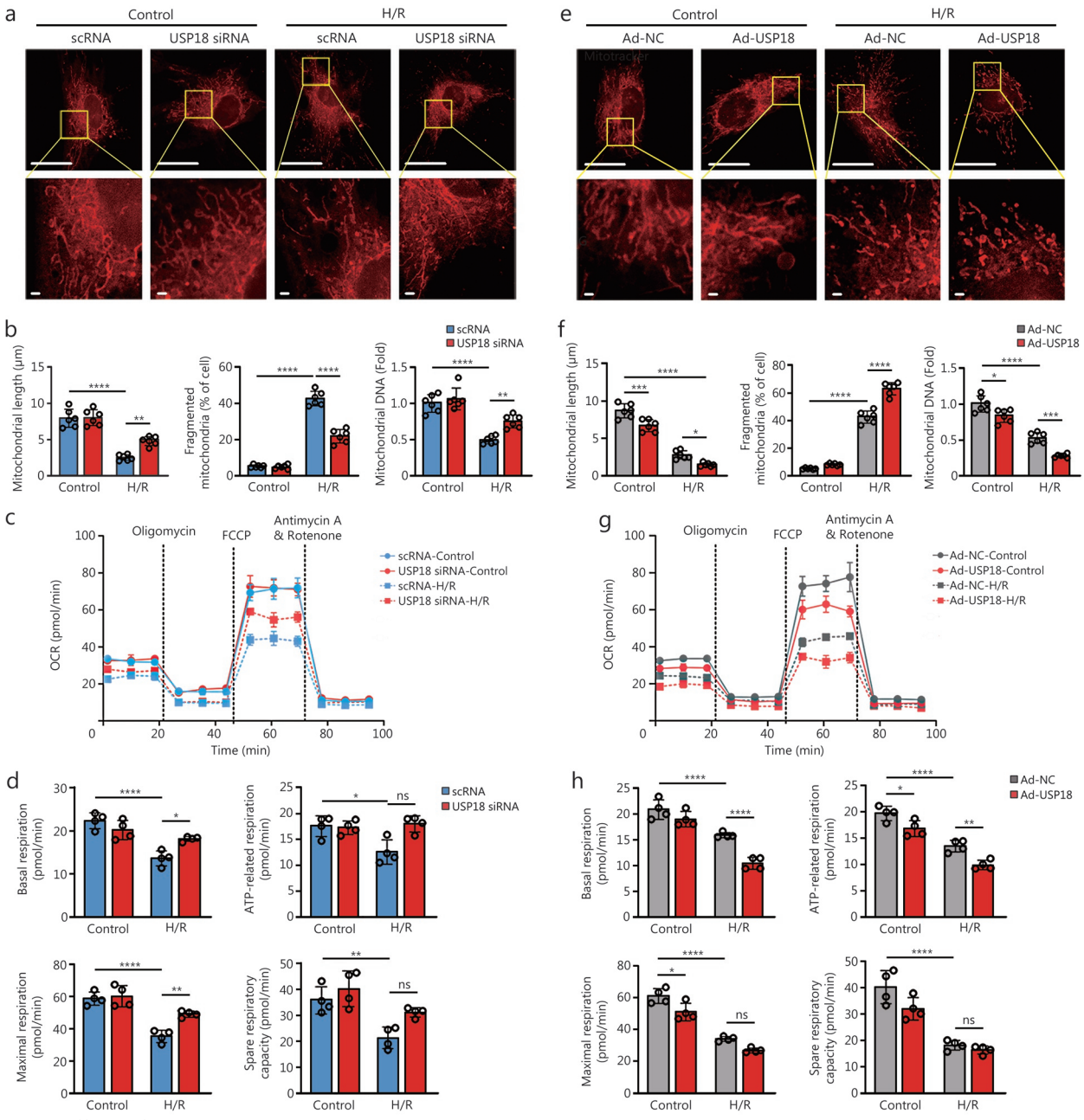

Fig. 4 Effects of USP18 on H/R-induced injury to NRVMs.

a-**d** NRVMs were transfected with USP18 siRNA and exposed to H/R. Scale bar=26 μm (top) and 50 μm (bottom). Representative confocal microscopy images showing mitochondrial morphology probed with MitoTracker Red (n=6) and quantification of mitochondrial length, mitochondrial fragmentation, and mitochondrial DNA levels (n=6) (**a** and **b**). Oxygen consumption rate (OCR) and quantitative statistical analysis of basal respiration, ATP-related respiration, maximal respiration, and spare respiratory capacity in NRVMs in the indicated groups (n=4) (**c** and **d**). **e**-**h** NRVMs were infected with Ad-USP18 and exposed to H/R. Scale bar=26 μm (top) and 50 μm (bottom). Representative confocal microscopy images showing mitochondrial morphology probed with MitoTracker Red (n=6) and quantification of mitochondrial length, mitochondrial fragmentation, and mitochondrial DNA levels (n=6) (**e** and **f**). Oxygen consumption rate (OCR) and quantitative statistical analysis of basal respiration, ATP-related respiration, maximal respiration, and spare respiratory capacity in NRVMs in the indicated groups (n=4) (**g** and **h**). *P<0.05, **P<0.01, ***P<0.001, ****P<0.0001, ns non-significant. USP18. Ubiquitin-specific protease 18; H/R. Hypoxia/reoxygenation; NC. Negative control; FCCP. Carbonyl cyanide p-trifluoromethoxyphenylhydrazone; NRVMs. Neonatal rat ventricular cardiomyocytes; ATP. Adenosine triphosphate; OCR. Oxygen consumption rate

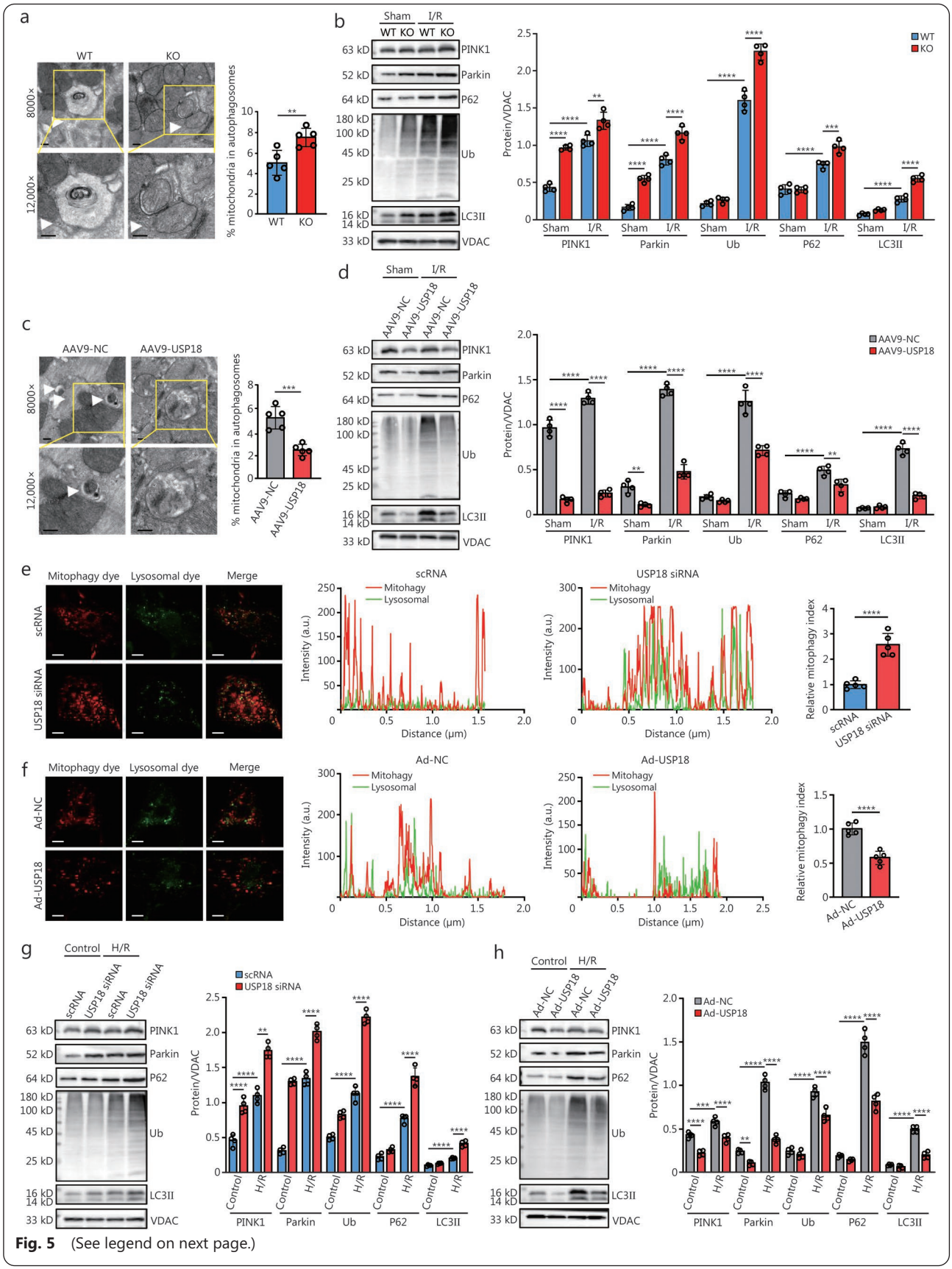

Fig. 5 (See legend on next page.)

(See figure on previous page.)

Fig. 5 USP18 aggravates cardiac I/R injury through regulation of mitochondria and inhibition of mitophagy.
a Electron microscopy image showing mitophagy in USP18-cKO mouse hearts (n=5). Scale bar=3 μm. White arrowheads indicate sites of mitophagy. **b** Protein levels of PINK1, Parkin, ubiquitinated proteins (Ub), P62, and LC3II in mitochondria from heart tissue in USP18-cKO and WT mice 24 h after I/R injury (n=4). **c** Electron microscopy image showing mitophagy in USP18-overexpress (OV) mouse hearts (n=5). Scale bar=3 μm. White arrowheads indicate sites of mitophagy. **d** Protein levels of PINK1, Parkin, Ub, P62, and LC3II proteins in mitochondria from the heart tissue of USP18-OV mice 24 h after I/R injury (n=4). Color shift in mitophagy dye (red) and lysosomal dye (green) in NRVMs showing mitophagy in NRVMs with USP18 siRNA transfection (**e**) or Ad-USP18 infection (**f**) and the quantitative mitophagy index in each group (n=5). Scale bar=9 μm. Protein levels of PINK1, Parkin, Ub, P62, and LC3II in mitochondria from NRVMs transfected with USP18 siRNA (**g**) or infected with Ad-USP18 (**h**). $^{**}P<0.01$, $^{***}P<0.001$, $^{****}P<0.0001$. USP18. Ubiquitin-specific protease 18; I/R. Ischemia/reperfusion; WT. Wild-type; KO. Knockout; P62. Sequestosome 1; LC3. Microtubule-associated protein 1 light chain 3; VDAC. Voltage-dependent anion channel

accumulation. USP18-cKO mice also exhibited reduced levels of proinflammatory cytokines (TNF-α, IL-1, IL-6) following myocardial I/R injury (Additional file 1: Fig. S6e). These findings suggest that USP18 may influence mitochondrial function primarily through mitophagy, which in turn affects the number of healthy mitochondria and mitochondrial respiration, oxidative stress, and apoptosis pathways.

Parkin knockdown in the heart aggravates acute cardiac I/R injury in USP18-cKO mice

To validate whether USP18 regulates cardiomyocyte injury through inhibition of mitophagy, NRVMs with silenced *USP18* were infected with Parkin siRNA to block mitophagy after H/R injury. As shown in Additional file 1: Fig. S7a, the Parkin siRNA exhibited an effective knockdown efficiency. The cellular protection from H/R injury observed with *USP18* silencing was significantly diminished by *Parkin* knockdown, as shown by reduced cell viability, increased LDH release, and increased DNA fragmentation and cleaved caspase-3 activity (Additional file 1: Fig. S7b). Additionally, the protective effects of *USP18* knockdown on H/R-induced mitochondrial injury in cardiomyocytes were diminished by *Parkin* silencing (Additional file 1: Fig. S7c, d). Similarly, *USP18* silencing-mediated cellular protection against H/R injury and mitochondrial dysfunction was also counteracted by Mdivi-1, a known inhibitor of mitochondrial fission, which is also an inhibitor of mitophagy [28] (Additional file 1: Fig. S8). Consistent with the *in vitro* findings, *in vivo Parkin* depletion exacerbated acute I/R-induced myocardial injury in USP18-cKO mice (Fig. 6a-d). Moreover, the protective effects of *USP18* knockout against I/R-induced acute cardiac injury, mitochondrial dysfunction, and mitophagy imbalance were significantly reversed by *Parkin* knockdown *in vivo* (Fig. 6b-h). In addition, the protective effects induced by USP18-cKO against adverse cardiac remodeling and cardiac dysfunction 4 weeks after I/R surgery were abolished by *Parkin* knockdown (Fig. 6i-l). These combined *in vivo* and *in vitro* findings suggest that impaired mitophagy is a key factor in USP18-mediated cardiac I/R injury.

USP18 inhibits mitophagy degradation and facilitates cardiac I/R injury through deubiquitinating and up-regulating PTEN-L

Immunoprecipitation coupled with mass spectrometry was used to identify candidate USP18-interacting partners involved in mitophagy regulation in cardiomyocytes. Following the removal of antibody-derived light and heavy chain peptides, we identified 138 potential target proteins of USP18, with PTEN ranking as the top hit (Additional file 1: Fig. S9a). A previous study has reported that, acting as a deubiquitinase, USP18 regulates the stability of PTEN in lung cancer cell lines [29]. Our findings revealed that the expression of PTEN-L, a newly identified isoform of PTEN, was downregulated in USP18-cKO hearts under both baseline and I/R stress conditions compared with that of full-length PTEN (Fig. 7a). Conversely, USP18-OV significantly increased the protein levels of PTEN-L but not those of PTEN in both baseline hearts and I/R-stressed hearts (Fig. 7b). In line with the *in vivo* results, PTEN-L expression was also downregulated by *USP18* knockdown but upregulated by USP18-OV in NRVMs under both baseline and I/R stress conditions (Additional file 1: Fig. S9b, c). Co-IP experiments further verified that USP18 interacted with PTEN-L but not with PTEN in NRVMs (Fig. 7c; Additional file 1: Fig. S9d, e). The endogenous interaction between USP18 and PTEN-L increased under both H/R (*in vitro*) and I/R (*in vivo*) conditions (Fig. 7d, e). PTEN-L ubiquitination was reduced following H/R and I/R (Fig. 7f). USP18 expression significantly decreased PTEN-L ubiquitination and increased PTEN-L protein levels in cell lysates, whereas *USP18* silencing led to increased PTEN-L ubiquitination and reduced PTEN-L protein levels under both control conditions and H/R conditions (Fig. 7g). No alterations in PTEN ubiquitination or protein expression were detected in cells overexpressing or lacking USP18 (Additional

file 1: Fig. S9f). To further elucidate the molecular domains responsible for the interaction between USP18 and PTEN-L, mutants of both proteins were constructed. Pull-down assays revealed that the 1–109 aa and 299–368 aa fragments of USP18 strongly associated with the ATR domain of PTEN-L (Fig. 7h, i). Furthermore, we discovered that USP18 significantly suppressed the Lys48-linked polyubiquitination of PTEN-L but not the Lys63-induced ubiquitination (Fig. 7j).

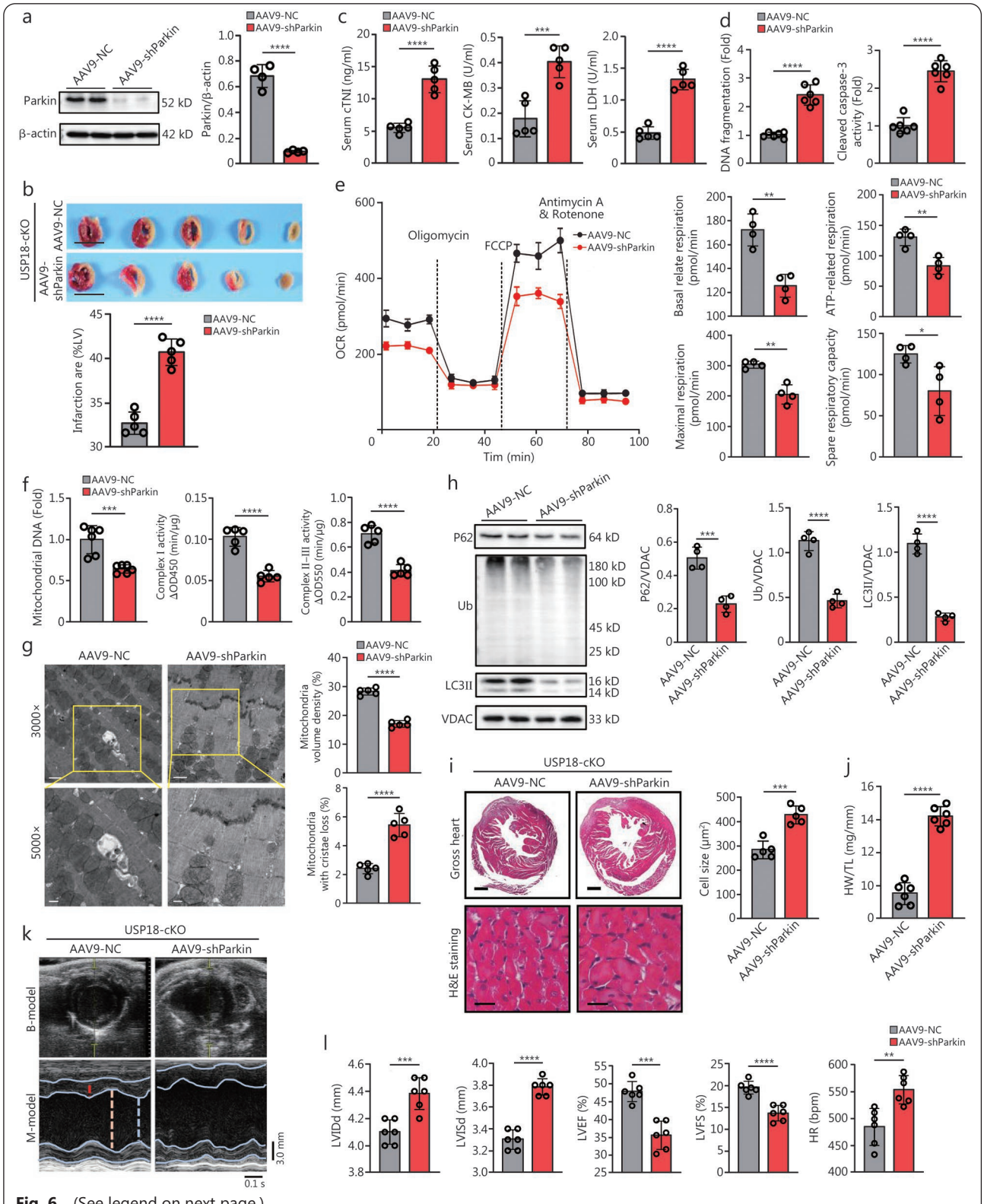

Fig. 6 (See legend on next page.)

(See figure on previous page.)

Fig. 6 *Parkin* knockdown counteracts the protection of *USP18* deficiency *in vivo*.

USP18-cKO mice were infected with AAV9-shParkin and subjected to I/R surgery. **a** Parkin protein levels in mouse hearts infected with AAV9-shParkin (n=4). **b** TTC staining of heart tissue 24 h post-I/R in each group (n=5). Scale bar=0.5 cm. **c** Serum levels of cTnI, CK-MB, and LDH in AAV9-shParkin-infected mice 4 h after I/R surgery (n=5). **d** DNA fragmentation and cleaved caspase-3 activity in heart tissue from AAV9-shParkin-infected mice 24 h after I/R injury (n=6). **e** Oxygen consumption rate (OCR) and quantitative statistical analysis of basal respiration, ATP-related respiration, maximal respiration, and spare respiratory capacity in mitochondria in the indicated groups (n=4). **f** Mitochondrial DNA (n=6) and complexes I and II–III activity (n=5) 24 h post-I/R in each group. **g** Representative electron microscopy images of heart sections 24 h post-I/R. The mitochondrial volume density and percent of mitochondria with cristae loss were measured in each group (n=5). Scale bar=10 μm (top) and 6 μm (bottom). **h** Protein levels of P62, ubiquitinated proteins (Ub), and LC3II in mitochondria from heart tissue 24 h after I/R injury (n=4). **i** H&E staining and quantitative statistical analysis of cell size (n=5) in USP18-cKO mice and AAV9-shParkin-infected mice 4 weeks after I/R injury. Scale bar=1 μm (top) and 50 μm (bottom). **j** Heart weight-to-tibia length ratio (HW/TL) (n=6) in each group. **k** Representative B-mode and M-mode echocardiographic images of the left ventricle from USP18-cKO mice and AAV9-shParkin-infected mice 4 weeks after I/R injury. **l** Cardiac function of USP18-cKO mice and AAV9-shParkin-infected mice 4 weeks after I/R injury (n=6). *P<0.05, **P<0.01, ***P<0.001, ****P<0.0001. USP18. Ubiquitin-specific protease 18; I/R. Ischemia/reperfusion; cTnI. Cardiac Troponin I; CK-MB. Creatine kinase-MB isoenzyme; LDH. Lactate dehydrogenase; NC. Negative control; AAV9. Adeno-associated virus serotype 9; AAV9-USP18. Adeno-associated virus serotype 9 encoding USP18; TTC. 2,3,5-triphenyltetrazolium chloride; ATP. Adenosine triphosphate; H&E. Hematoxylin and eosin; PSR. Picrosirius red; FCCP. Carbonyl cyanide p-trifluoromethoxyphenylhydrazone; LVIDd. Left ventricle internal diameter at diastole; LVISd. Left ventricle internal diameter at systole; LVEF. Left ventricle ejection fraction; LVFS. Left ventricle fractional shortening; HR. Heart rate

NRVMs were treated with cycloheximide to inhibit protein translation. We observed that *USP18* silencing markedly reduced the half-life of the PTEN-L protein, whereas the half-life increased in NRVMs infected with Ad-USP18 (Fig. 7k, l). These findings suggest that USP18 stabilizes PTEN-L by specifically binding and deubiquitinating it. Phosphorylated ubiquitin at Ser65 (pSer65-Ub) directly engages Parkin, facilitating its translocation from the cytosol to mitochondria [30]. PTEN-L directly dephosphorylates pSer65-Ub, thereby decreasing its mitochondrial level [11]. To investigate whether USP18 regulates mitophagy through the PTEN-L-pSer65-Ub-Parkin pathway, we evaluated the effect of pSer65-Ub on mitochondria in I/R-stressed hearts and NRVMs. As anticipated, the protein level of pSer65-poly-Ub was elevated in USP18-cKO mouse hearts and cardiomyocytes (Additional file 1: Fig. S10a, b), whereas it was decreased in USP18-OV mouse hearts and cardiomyocytes (Additional file 1: Fig. S10a, b). Moreover, we also observed an interaction between PTEN-L and Parkin in cardiomyocytes (Additional file 1: Fig. S10c, d). USP18 overexpression increased the cellular interaction between PTEN-L and Parkin, whereas *USP18* silencing reduced the PTEN-L-Parkin interaction under H/R (Additional file 1: Fig. S10e). USP18-cKO significantly reduced the PTEN-L-Parkin interaction after I/R. Conversely, USP18 overexpression increased this interaction in post-I/R hearts (Additional file 1: Fig. S10f). However, PTEN-L inhibited the translocation of Parkin from the cytoplasm to the mitochondria (Additional file 1: Fig. S10g). Moreover, a Phos-tag assay revealed that PTEN-L reduced p-Parkin levels in NRVMs treated with carbonyl cyanide m-chlorophenyl hydrazone (CCCP) (Additional file 1: Fig. S10h). Collectively, these findings suggest that by deubiquitinating PTEN-L, USP18 increases the level of PTEN-L in cardiomyocytes during I/R stress and that PTEN-L interacts with Parkin, subsequently inhibiting its phosphorylation and translocation into mitochondria, thus suppressing mitophagy degradation.

To directly assess whether the detrimental effects of USP18 on cardiomyocytes are dependent on its deubiquitinase activity, we constructed a catalytically inactive mutant of USP18 (C61A). Overexpression of WT USP18 significantly exacerbated mitochondrial dysfunction and cell injury under H/R conditions. In contrast, the USP18-C61A mutant [31], which lacks deubiquitinase activity, failed to reproduce these effects (Additional file 1: Fig. S11a, b). These results strongly support the conclusion that the deleterious effects of USP18 on cardiomyocytes are mediated primarily through its deubiquitinase activity. A previous study reported that the phosphatase domain of PTEN-L is essential for its interaction with Parkin [11]. To investigate this further, we constructed a phosphatase-deficient mutant of PTEN-L (PTEN-L-C297S), as described previously [11]. Overexpression of WT PTEN-L significantly exacerbated mitochondrial dysfunction and cell injury under H/R conditions. In contrast, the *PTEN-L-C297S* mutant failed to replicate these effects, indicating that the phosphatase activity of PTEN-L is required for its detrimental role in mitochondrial homeostasis (Additional file 1: Fig. S11c).

We then transfected USP18-OV NRVMs with PTEN-L siRNA, which specifically knocked down *PTEN-L* without

affecting canonical PTEN protein levels (Additional file 1: Fig. S12a). PTEN-L suppression significantly reduced H/R-induced cell injury, improved mitochondrial function, and restored mitophagy. However, USP18 overexpression did not counteract the cellular protection against H/R injury caused by *PTEN-L* knockdown (Additional file 1: Fig. S12b-d). We then infected *USP18*-silenced NRVMs with an adenovirus encoding PTEN-L (Ad-PTEN-L), which specifically overexpressed PTEN-L without affecting canonical PTEN protein levels (Additional file 1: Fig. S13a). PTEN-L overexpression significantly aggravated I/R-induced acute cell injury, mitochondrial dysfunction, and impaired mitophagy.

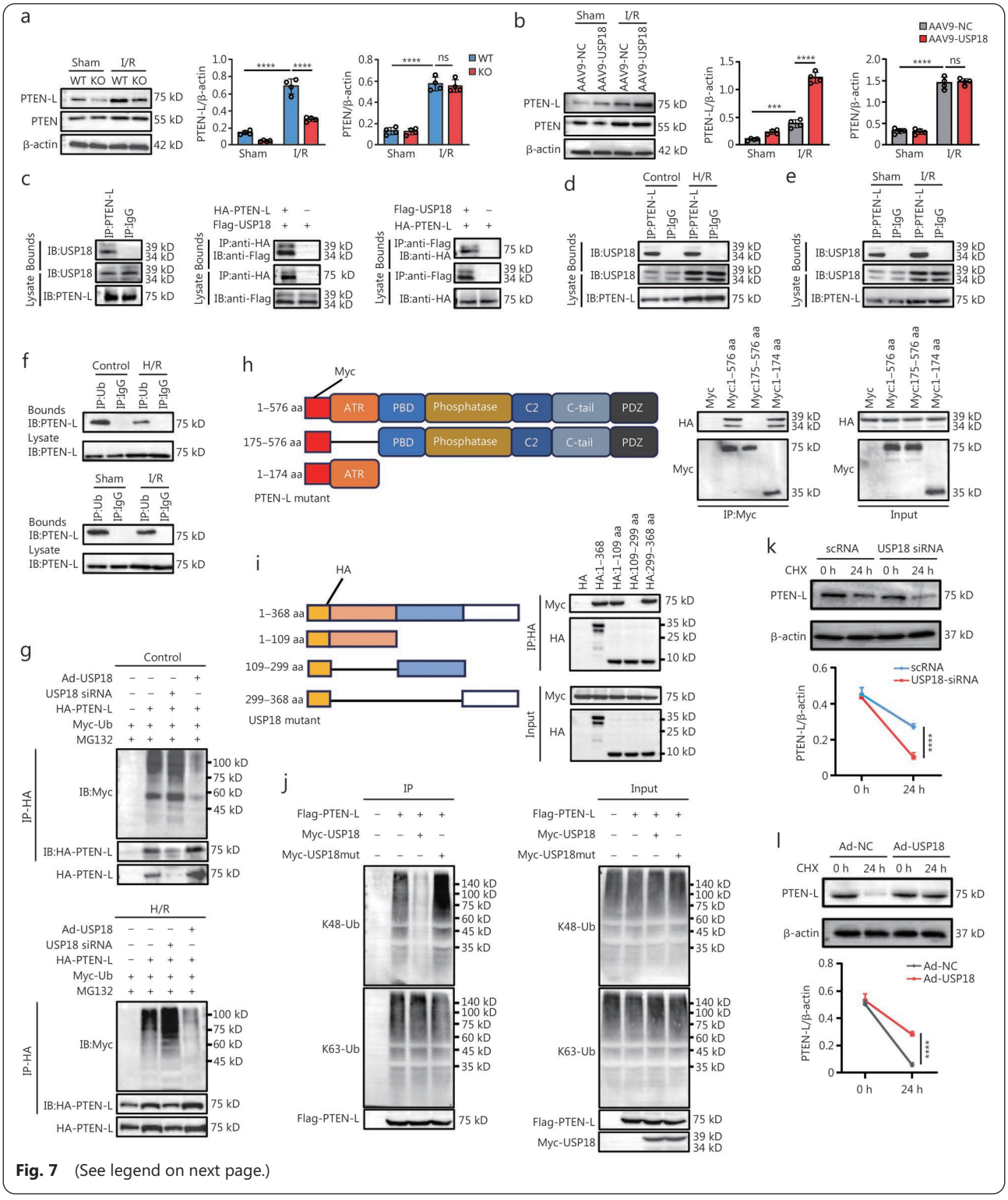

Fig. 7 (See legend on next page.)

(See figure on previous page.)

Fig. 7 USP18 inhibits mitophagy degradation and facilitates cardiac I/R injury through deubiquitinating and upregulating PTEN-L.

a The protein levels of PTEN-L and PTEN in USP18-cKO mouse hearts 24 h after I/R injury (n=4). ****P<0.0001, ns non-significant. **b** The protein levels of PTEN-L and PTEN in AAV9-USP18-infected mouse hearts 24 h after I/R injury (n=4). ***P<0.001, ****P<0.0001, ns non-significant. **c** Co-IP of USP18 and PTEN-L in NRVMs (left); NRVMs were transfected with HA-PTEN-L and Flag-USP18 (middle); Co-IP of Flag-USP18 and HA-PTEN-L in NRVMs (right). **d** Endogenous Co-IP of USP18 and PTEN-L in NRVMs subjected to H/R injury. **e** Endogenous Co-IP of USP18 and PTEN-L in hearts subjected to I/R injury. **f** PTEN-L ubiquitination (Ub) levels assessed by CO-IP in NRVMs subjected to H/R injury (top) and hearts subjected to I/R injury (bottom). **g** NRVMs were transfected with Ad-USP18 or USP18 siRNA or HA-PTEN-L and Myc-Ub and treated with MG132. Co-IP of Myc-Ub and HA-PTEN-L. **h** Schematic representations of the domains of PTEN-L involved in binding to USP18. Full-length PTEN-L or truncated PTEN-L was coexpressed with USP18 in HEK293T cells. Cells were subjected to immunoprecipitation with an anti-Myc antibody or an anti-HA antibody, followed by immunoblotting with the indicated antibodies. **i** Schematic representations of USP18 residues involved in binding to PTEN-L. Full-length USP18 or USP18 truncations were coexpressed with PTEN-L in HEK293T cells. Cells were subjected to immunoprecipitation with an anti-Myc antibody or an anti-HA antibody, followed by immunoblotting with the indicated antibodies. **j** Ub assay of PTEN-L in HEK293T cells cotransfected with Myc-USP18, Myc-USP18-mut, and Flag-PTEN-L and treated with 10 μmol/L MG132. **k**, **l** NRVMs were transfected with scRNA or USP18 siRNA (**k**), infected with Ad-NC or Ad-USP18 (**l**), and then treated with cycloheximide (CHX, 10 μmol/L) for the indicated time periods. Representative immunoblot analysis of PTEN-L protein levels in each group. ****P<0.0001 vs. scRNA or Ad-NC. USP18. Ubiquitin-specific protease 18; I/R. Ischemia/reperfusion; H/R. Hypoxia-reoxygenation; PTEN. Phosphatase and tensin homolog; PTEN-L. Phosphatase and tensin homolog-long; AAV9. Adeno-associated virus serotype 9; NC. Negative control

However, *USP18* knockdown did not abolish the adverse effects of PTEN-L overexpression on H/R injury (Additional file 1: Fig. S13b-d). Mice were injected with AAV9-shPTEN-L to specifically knock down PTEN-L *in vivo* without altering canonical PTEN protein levels (Additional file 1: Fig. S14a). *PTEN-L* knockdown in hearts attenuated acute cardiac I/R injury (Additional file 1: Fig. S14a-c), mitochondrial dysfunction (Additional file 1: Fig. S14d, e), mitophagy imbalance (Additional file 1: Fig. S14f, g), long-term adverse cardiac remodeling (Additional file 1: Fig. S14h, i), and cardiac dysfunction (Additional file 1: Fig. S14j, k). The overexpression of USP18 did not lead to worsened cardiac I/R injury, mitochondrial dysfunction, or adverse remodeling in mice lacking PTEN-L (Additional file 1: Fig. S14b-l).

An anti-PTEN-L antibody protects against cardiac I/R injury *in vivo*

PTEN-L, a secreted protein, has been detected in human serum and plasma [32]. To further investigate this phenomenon, we measured serum PTEN-L levels in mice subjected to I/R stress. Additional file 1: Fig. S15a, b demonstrates that I/R challenge led to an increase in the level of circulating PTEN-L. The serum level of PTEN-L increased in USP18-OV mice but decreased in USP18-cKO mice (Additional file 1: Fig. S15a, b). Consistently, we also found that the level of PTEN-L increased in the supernatant of USP18-OV NRVMs but decreased in the supernatant of *USP18*-silenced NRVMs (Additional file 1: Fig. S15c, d). The ATR of PTEN-L facilitates its secretion from donor cells and uptake by recipient cells [32]. We subsequently infected NRVMs with Ad-PTEN-L containing a mutated ATR region [Ad-PTEN-L (ATR-MUT)]. PTEN-L is an isoform of canonical PTEN and is characterized by the addition of an ATR region at the N-terminus of PTEN [32]. Thus, we assessed the expression of PTEN-L (ATR-MUT) with an anti-PTEN antibody. The level of PTEN-L in the supernatant of cardiomyocytes was abolished in NRVMs infected with Ad-PTEN-L (ATR-MUT) (Additional file 1: Fig. S16a, b). No aggravating effects on H/R-induced mitochondrial dysfunction or cell injury were observed following treatment with Ad-PTEN-L (ATR-MUT) (Additional file 1: Fig. S16c, d). To further investigate whether PTEN-L exerts its deleterious effects through paracrine signaling, we collected conditioned medium from H/R-injured cardiomyocytes transfected with Ad-NC or Ad-PTEN-L and applied it to cardiomyocytes. Interestingly, exposure to PTEN-L-rich conditioned media resulted in decreased H/R injury and mitochondrial DNA levels (Additional file 1: Fig. S17a, b). Furthermore, this PTEN-L-rich conditioned media significantly aggravated H/R injury in *PTEN-L*-silenced cells (Additional file 1: Fig. S17a, b). The potential therapeutic effect of a PTEN-L neutralizing antibody against cardiac I/R injury was subsequently investigated. As anticipated, treatment with the antibody mitigated the detrimental effect of H/R on NRVMs (Additional file 1: Fig. S17b). To validate the protective effects of the antagonistic anti-PTEN-L antibody, mice were injected with the anti-PTEN-L antibody after cardiac I/R surgery. The anti-PTEN-L antibody significantly protected against acute cardiac I/R injury (Additional file 1: Fig. S18a, b), mitochondrial dysfunction (Additional file 1: Fig. S18c-e), mitophagy imbalance (Additional file 1:

Fig. S18f, g), adverse cardiac remodeling, and cardiac dysfunction (Additional file 1: Fig. S18h-k). Taken together, our *in vivo* and *in vitro* results indicate that elevated serum PTEN-L in cardiomyocytes contributes to the detrimental effects of USP18 on cardiac I/R injury.

We evaluated serum PTEN-L levels in patients with ST-segment elevation myocardial infarction (STEMI) and in healthy control individuals. As depicted in Additional file 1: Fig. S17c, serum PTEN-L levels increased in patients with STEMI and further increased in the serum of STEMI patients immediately after PCI. We also explored the association of PTEN-L levels with cardiac function in all control and STEMI patients post-PCI. As a result, the PTEN-L level post PCI was negatively related to LVEF (R^2=0.7233, P<0.0001). Negative correlation was found with LVFS (R^2=0.7389, P<0.0001) (Additional file 1: Fig. S17d). The clinical characteristics are listed in Additional file 1: Table S2. Our data indicate that cardiac I/R injury upregulates USP18 in the heart, which binds PTEN-L to inhibit Parkin phosphorylation and mitochondrial translocation, thereby suppressing mitophagy and exacerbating myocardial injury. PTEN-L further promotes cardiac damage via a paracrine mechanism, and targeting the USP18-PTEN-L axis restores mitophagy and protects the heart (Fig. 8).

Discussion

The advent of revascularization therapy has significantly affected the clinical landscape of coronary heart disease. Despite advancements in and widespread application of coronary reperfusion interventions, AMI still has a significant burden of morbidity and mortality [4]. Various types of cardiomyocyte death and coronary microvascular injury are induced by persistent I/R, contributing significantly to the onset of heart failure [5]. Therefore, reducing revascularization-induced cardiac injury represents a neglected therapeutic target but remains an unmet clinical need [5]. In this study, we revealed a previously unreported molecular signature in postreperfusion hearts characterized by marked induction of USP18 expression. Notably, suppressing USP18 effectively protected against cardiac injury, mitochondrial dysfunction, cardiac dysfunction, cardiac remodeling,

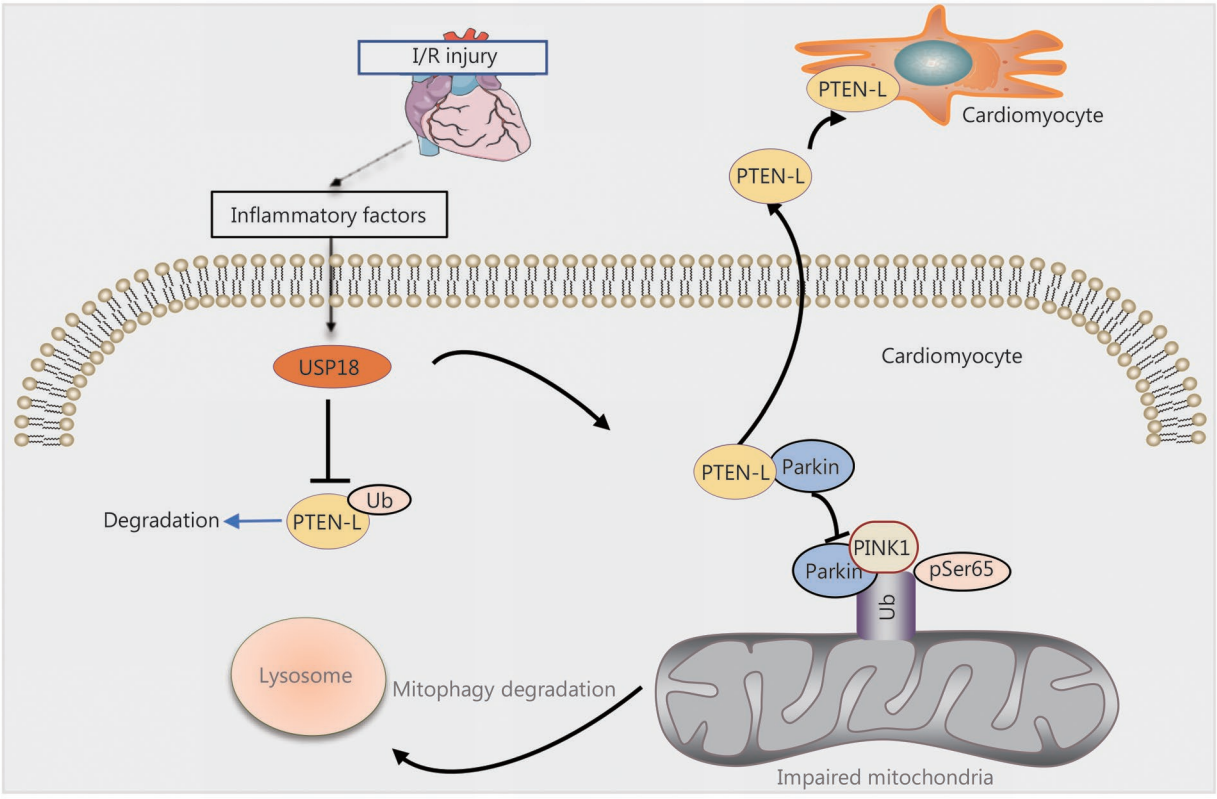

Fig. 8 Summary of the key findings in this paper.
Cardiac I/R injury upregulates USP18 in both mouse and human hearts. USP18 interacts with PTEN-L, inhibiting Parkin phosphorylation and mitochondrial translocation, thereby suppressing mitophagy and exacerbating mitochondrial dysfunction and myocardial injury. PTEN-L additionally promotes cardiac damage via a paracrine mechanism. Genetic or pharmacological targeting of the USP18-PTEN-L axis restores mitophagy and protects against I/R-induced cardiac injury, representing a potential therapeutic strategy. I/R. Ischemia/reperfusion; PTEN-L. Phosphatase and tensin homolog-long; USP18. Ubiquitin-specific protease 18; Ub. Ubiquitination

and heart failure in mice. The upregulation of USP18 was found to be sufficient to worsen cardiac I/R injury in both experimental models and cultured cells. Mechanistically, the upregulated deubiquitinase USP18 in I/R-injured hearts directly bound to PTEN-L and inhibited its ubiquitination-mediated degradation. Consequently, this suppressed Parkin translocation to mitochondria and mitigated pSer65-Ub levels, leading to impaired mitophagy. These events collectively facilitated cardiac I/R injury.

USP18 has long been recognized as an ISGylation-specific member of the deubiquitinase family and is responsible for removing interferon-stimulated gene 15 (ISG15) or ubiquitin from conjugated proteins in a manner dependent on its deconjugating activity [26]. The deubiquitinase activity of USP18 is a crucial component underlying its pathophysiological functions, including those in immune diseases and tumorigenesis [26]. USP18 is involved in numerous physiological processes, yet its precise contribution to cardiovascular disease is still unclear. USP18 exerts protective effects against pressure overload-induced cardiac remodeling by targeting the transforming growth factor-β-activated kinase 1-p38/c-Jun N-terminal kinase signaling cascade [19]. Positive associations between circulating USP18 concentrations and systolic blood pressure, pulse pressure, and heart rate were identified by Dziamałek-Macioszczyk *et al*. [33]. In this study, we also detected increased USP18 expression in patients with IHD, in murine hearts subjected to I/R injury, and in cardiomyocytes exposed to I/R conditions. In contrast to the findings of the aforementioned study, our findings revealed that USP18 overexpression exacerbated mitochondrial dysfunction, aggravated cardiac I/R injury, and worsened cardiac remodeling and dysfunction. The key differences lie in the pathophysiological context and cellular stress involved. The angiotensin II model involves primarily hypertrophic signaling and fibrotic remodeling, whereas I/R injury is characterized by acute oxidative stress, mitochondrial dysfunction, and mitophagy activation. Our data revealed that under I/R stress, USP18 impaired mitochondrial quality control by inhibiting mitophagy, thereby aggravating injury. These findings suggest that USP18 may act in a stimulus-specific and pathway-dependent manner; it may be beneficial in certain chronic remodeling settings but detrimental in acute ischemic injury because it can compromise mitochondrial homeostasis.

Mitochondria are vital for sustaining cardiac homeostasis, as they supply the major energy needed for excitation-contraction coupling in the heart. Additionally, mitochondria regulate critical intracellular survival and cell death pathways [6,34]. Programmed mitophagy is critical in physiological settings where the deliberate removal of mitochondria is necessary for developmental processes [5,34]. In response to stress, mitophagy regulates cellular metabolism, particularly during external insults. Emerging evidence highlights its role in cardiac I/R injury, as dysregulated mitophagy leads to the accumulation of dysfunctional mitochondria, impaired ATP production, mitochondrial dysfunction, and metabolic disorders. This dysregulation further contributes to oxidative stress, cell death, and, subsequently, pathological cardiac remodeling and heart failure [35-37]. Previously, Ma *et al*. [38] reported that USP18 promotes resistance to vemurafenib in B-Raf proto-oncogene, serine/threonine kinase V600E-mutant melanoma cells by regulating autophagy. Our RNA-seq results revealed that the mitochondrial metabolism pathway was the top signaling pathway altered in *USP18*-deficient hearts. Additionally, we found that during I/R injury, USP18 suppressed mitophagy degradation, resulting in increased accumulation of impaired mitochondria in cardiomyocytes, which exacerbated mitochondrial dysfunction. Among known mitophagy pathways, the Parkin-dependent mechanism has been the most extensively characterized [8]. Following mitochondrial damage, PINK1 is recruited to and activated on the outer mitochondrial membrane, subsequently phosphorylating mitochondrial ubiquitin at Ser65 [8,30]. By acting as a critical signal, pSer65-Ub recruits cytosolic Parkin to the outer mitochondrial membrane, thereby promoting the elimination of damaged mitochondria and supporting mitochondrial homeostasis [8,39]. Other signaling molecules, such as FUN14 domain-containing 1 and BCL2/adenovirus E1B 19 kD interacting protein 3, also act as mitophagy receptors to regulate mitophagy [40,41]. Our results revealed that USP18 downregulated mitochondrial PINK1 and Parkin levels during I/R injury, whereas the expression of FUN14 domain-containing 1 and BCL2/adenovirus E1B 19 kD interacting protein 3 remained unaffected. *USP18* deficiency increased the cardiac and cardiomyocyte levels of PINK1 and Parkin in mitochondria during I/R injury. Treatment with a mitophagy inhibitor or knockdown of *Parkin* in cardiomyocytes dramatically inhibited USP18-cKO-mediated cardioprotection. These results suggest that USP18 functions as a modulator of the PINK1/Parkin-mediated mitophagy pathway in the context of cardiac I/R injury.

The tumor suppressor PTEN is known to suppress the class I phosphoinositide 3-kinase-protein kinase B-mechanistic target of rapamycin (PI3K-Akt-mTOR) signaling cascade and may also affect autophagic processes through its effect on Akt activity [42]. Mustachio *et al*. [29] recently reported that

USP18 influences carcinogenesis through its regulation of PTEN stability in lung cancer cell models. However, we found that USP18 regulated the stability of PTEN-L but not PTEN in cardiomyocytes. Encoded by the same mRNA as PTEN, PTEN-L possesses an N-terminal ATR that facilitates its intercellular transfer via secretion and uptake mechanisms [32]. Research has revealed that PTEN-L is a mitochondrial protein that regulates mitochondrial energy metabolism [43]. Wang *et al*. [11] reported that PTEN-L utilizes its protein phosphatase function to dephosphorylate pSer65-Parkin, thus blocking the autoubiquitination of Parkin and inhibiting mitophagy in HeLa cells. Our findings revealed that USP18 selectively bound to PTEN-L but not to PTEN and protected it from ubiquitin-dependent degradation. Increased levels of USP18 led to elevated levels of PTEN-L, which could also bind to Parkin in the cytoplasm to suppress Parkin phosphorylation and translocation to mitochondria in cardiomyocytes. Moreover, we also revealed that USP18 reduced the level of pSer65-Ub, which may have facilitated the suppression of PINK1-Parkin-mediated mitophagy degradation. Moreover, knockdown of *PTEN-L* reversed USP18 overexpression-induced cardiac injury, mitochondrial dysfunction, and cardiac dysfunction. Collectively, these results suggest that USP18 may serve as a detrimental modulator of mitophagy during myocardial I/R injury.

Secreted PTEN-L has been shown to modulate key oncogenic processes, including cell proliferation, motility, and invasive capacity, in cancer cells [44]. In this study, we found that serum PTEN-L was upregulated in STEMI patients and further increased in the serum of STEMI patients after PCI surgery. Notably, the administration of an anti-PTEN-L antagonistic antibody effectively attenuated mitochondrial dysfunction, adverse remodeling, and cardiac impairment induced by I/R injury. These findings suggest that the upregulation of PTEN-L by USP18 may suppress PINK1-Parkin-mediated mitophagy in cardiomyocytes through both intracellular and paracrine mechanisms. Although the precise mechanism remains to be fully elucidated, this paracrine effect may involve the uptake of extracellular PTEN-L, which impairs the recruitment of Parkin to damaged mitochondria. USP18 expression is strongly upregulated by type I and type III interferons and other inflammatory factors, such as TNF-α and lipopolysaccharides [26]. Consistently, we found that the upregulation of USP18 in cardiomyocytes during cardiac I/R stress was associated with inflammation. Treatment with a TNF-α antibody or an HMGB1 antibody dramatically inhibited the I/R-induced upregulation of USP18 and PTEN-L expression.

In this study, we used a single dose of AAV9-USP18 that resulted in an overexpression level comparable to the endogenous increase observed after myocardial I/R injury. This design was intended to closely mimic the pathological upregulation of USP18 under disease conditions. However, we acknowledge that the use of a single expression level limits our ability to determine whether USP18 exerts graded or threshold-dependent effects on mitochondrial function, inflammation, or cardiac injury. Future studies incorporating a dose-response approach with varied titers of AAV9-USP18 will be important to define the functional range and therapeutic window of USP18 modulation in the heart. Short-term administration of a PTEN-L-neutralizing antibody conferred cardioprotection after myocardial I/R injury, but the long-term safety and clinical applicability of PTEN-L blockade warrant further investigation. Although the antibody used was designed to specifically target the N-terminal extension unique to PTEN-L and did not alter canonical PTEN expression in our models, off-target effects and immune responses remain possible. Therefore, future studies are needed to assess the pharmacokinetics, isoform selectivity, and long-term effects of PTEN-L inhibition *in vivo*. Potential off-target effects of USP18 manipulation were minimized by cardiomyocyte-specific strategies, although indirect effects on other pathways cannot be completely excluded and warrant further investigation.

Conclusions

In summary, during I/R injury, USP18 upregulation by inflammatory factors reduced ubiquitination degradation and increased the level of PTEN-L. PTEN-L, in turn, binds to Parkin in the cytoplasm, suppressing Parkin translocation to mitochondria, thereby inhibiting mitophagy degradation and subsequently accelerating cardiac injury. USP18 was identified as a harmful factor enriched in cardiomyocytes and associated with inflammation, suggesting that therapeutic targeting of the USP18/PTEN-L pathway may offer a promising strategy for alleviating cardiac I/R injury.

Abbreviations

AAV9: Adeno-associated virus serotype 9
AMI: Acute myocardial infarction
ATR: Alternatively translated region
CK-MB: Creatine kinase-MB isoenzyme
cTnI: Cardiac troponin I
cTnT: Cardiac troponin T
GO: Gene Ontology
HMGB1: High mobility group box 1
H/R: Hypoxia/reoxygenation
IHD: Ischemic heart disease
IL: Interleukin
I/R: Ischemia/reperfusion

LDH: Lactate dehydrogenase
LV: Left ventricle
NRVMs: Neonatal rat ventricular cardiomyocytes
OCR: Oxygen consumption rate
OV: Overexpression
PGC-1α: Peroxisome proliferator-activated receptor gamma coactivator-1α
PCI: Percutaneous coronary intervention
PINK1: PTEN-induced putative kinase 1
PTEN-L: Phosphatase and tensin homolog-long
pSer65-Ub: Phosphorylated ubiquitin at serine 65
ROS: Reactive oxygen species
STEMI: ST-segment elevation myocardial infarction
TFAM: Mitochondrial transcription factor A
TNF-α: Tumor necrosis factor-α
USP18: Ubiquitin-specific protease 18
WT: Wild-type.

Supplementary information

The online version contains supplementary material available at https://doi.org/10.1016/j.mmr.2026.100004.

Additional file 1. Methods. Fig. S1 USP18 expression is induced by cardiac I/R injury. **Fig. S2** *USP18* deficiency mitigates cardiac remodeling and dysfunction following cardiac I/R injury. **Fig. S3** Cardiac-specific overexpression of USP18 aggravates I/R-induced mitochondrial dysfunction and acute cardiac injury in mice. **Fig. S4** The effects of USP18 on hypoxia/reoxygenation (H/R) induced cell injury in NRVMs. **Fig. S5** USP18 aggravates cardiac I/R injury through regulating mitochondria and inhibiting mitophagy. **Fig. S6** Effects of USP18 on other mitochondrial processes. **Fig. S7** *Parkin* knockdown counteracts the protection of *USP18* deficiency *in vitro*. **Fig. S8** Mitophagy inhibitor Mdivi-1 counteracts the protection of *USP18* deficiency *in vitro*. **Fig. S9** USP18 inhibits mitophagy degradation and facilitates cardiac I/R injury through deubiquitinating and upregulating PTEN-L. **Fig. S10** USP18 inhibits mitochondria pSer65-poly-Ub and Parkin. **Fig. S11** *USP18-C61A* mutant failed to exert adverse effects *in vitro*. **Fig. S12** *PTEN-L* knockdown mimics the effects of USP18 overexpression *in vitro*. **Fig. S13** PTEN-L overexpression abolishes the effects of *USP18* knockdown *in vitro*. **Fig. S14** *PTEN-L* knockdown counteracts the protective effect of *USP18* overexpression *in vivo*. **Fig. S15** Serum PTEN-L level in *USP18* deficiency or overexpression mice. **Fig. S16** The effects of PTEN-L are abolished by *PTEN-L ATR*-mutant, PTEN-L antibody protects against H/R-induced cell injury *in vitro*. **Fig. S17** USP18 is upregulated in the serum of AMI patients. **Fig. S18** An anti-PTEN-L antibody protects against cardiac I/R injury *in vivo*. **Table S1** Primer sequences for RT-PCR. **Table S2** Clinical characteristics and myocardial biomarker levels of individuals included in the metabolomics assay.

Acknowledgements

We acknowledge American Journal Experts (AJE) for manuscript language polishing.

Authors' contributions

QQW and YX drafted the manuscript. YYH, XYY, XYY, KQD, ZLJ, WZ, and JLC collected the data. LHN and YZF analyzed the data. QQW and YX wrote and revised the manuscript. QQW and XRH received the funding for this study. ZBL and XRH gave administrative or logistic support for this review. All authors read and approved the final manuscript.

Funding

This work was supported by the National Natural Science Foundation of China (82470399, 82170382, 82400401, and 82370290), and the Wuhan University Zhongnan Hospital Translational Medicine and Interdisciplinary Research Joint Fund (ZNJC202308).

Availability of data and materials

The findings of this study are supported by data available from the corresponding authors upon reasonable request.

Declarations

Ethics approval and consent to participate

All experimental protocols received approval from the Animal Care and Use Committee at Zhongnan Hospital of Wuhan University (ZN2023201). For procedures involving human samples, compliance with the Declaration of Helsinki was ensured, and approval was granted by the Review Board of Zhongnan Hospital of Wuhan University (2025058K). Written informed consent was obtained from all patients and donors involved.

Consent for publication

Not applicable.

Competing interests

The authors declare that they have no competing interests.

Author details

[1]Department of Cardiology, Zhongnan Hospital of Wuhan University, Wuhan 430062, China. [2]Institute of Myocardial Injury and Repair, Wuhan University, Wuhan 430062, China. [3]Department of Cardiology, Renmin Hospital of Wuhan University, Cardiovascular Research Institute, Wuhan University, Wuhan 430060, China.

References

1. Dauerman HL, Ibanez B. The edge of time in acute myocardial infarction. J Am Coll Cardiol. 2021;77(15):1871-4.
2. Bahit MC, Kochar A, Granger CB. Post-myocardial infarction heart failure. JACC Heart Fail. 2018;6(3):179-86.
3. Ibanez B, James S, Agewall S, Antunes MJ, Bucciarelli-Ducci C, Bueno H, *et al*. 2017 ESC Guidelines for the management of acute myocardial infarction in patients presenting with ST-segment elevation. Rev Esp Cardiol (Engl Ed). 2017;70(12):1082.
4. Algoet M, Janssens S, Himmelreich U, Gsell W, Pusovnik M, Van den Eynde J, *et al*. Myocardial ischemia-reperfusion injury and the influence of inflammation. Trends Cardiovasc Med. 2023;33(6):357-66.
5. Zhou M, Yu Y, Luo X, Wang J, Lan X, Liu P, *et al*. Myocardial ischemia-reperfusion injury: therapeutics from a mitochondria-centric perspective. Cardiology. 2021;146(6):781-92.
6. Yang M, Linn BS, Zhang Y, Ren J. Mitophagy and mitochondrial integrity in cardiac ischemia-reperfusion injury. Biochim Biophys Acta Mol Basis Dis. 2019;1865(9):2293-302.
7. Cai C, Guo Z, Chang X, Li Z, Wu F, He J, *et al*. Empagliflozin attenuates cardiac microvascular ischemia/reperfusion through activating the AMPKα1/ULK1/FUNDC1/mitophagy pathway. Redox Biol. 2022;52:102288.
8. Narendra DP, Youle RJ. The role of PINK1-Parkin in mitochondrial quality control. Nat Cell Biol. 2024;26(10):1639-51.

9. Ai L, de Freitas Germano J, Huang C, Aniag M, Sawaged S, Sin J, *et al*. Enhanced Parkin-mediated mitophagy mitigates adverse left ventricular remodelling after myocardial infarction: role of PR-364. Eur Heart J. 2025;46(4):380-93.
10. Kubli DA, Zhang X, Lee Y, Hanna RA, Quinsay MN, Nguyen CK, *et al*. Parkin protein deficiency exacerbates cardiac injury and reduces survival following myocardial infarction. J Biol Chem. 2013;288(2):915-26.
11. Wang L, Cho YL, Tang Y, Wang J, Park JE, Wu Y, *et al*. PTEN-L is a novel protein phosphatase for ubiquitin dephosphorylation to inhibit PINK1-Parkin-mediated mitophagy. Cell Res. 2018;28(8): 787-802.
12. Zhang N, Zhang Y, Qian H, Wu S, Cao L, Sun Y. Selective targeting of ubiquitination and degradation of PARP1 by E3 ubiquitin ligase WWP2 regulates isoproterenol-induced cardiac remodeling. Cell Death Differ. 2020;27(9):2605-19.
13. Popovic D, Vucic D, Dikic I. Ubiquitination in disease pathogenesis and treatment. Nat Med. 2014;20(11):1242-53.
14. Niu K, Fang H, Chen Z, Zhu Y, Tan Q, Wei D, *et al*. USP33 de-ubiquitinates PRKN/Parkin and antagonizes its role in mitophagy. Autophagy. 2020;16(4):724-34.
15. Xie SY, Liu SQ, Zhang T, Shi WK, Xing Y, Fang WX, *et al*. USP28 serves as a key suppressor of mitochondrial morphofunctional defects and cardiac dysfunction in the diabetic heart. Circulation. 2024;149(9):684-706.
16. Zhang M, Zhang MX, Zhang Q, Zhu GF, Yuan L, Zhang DE, *et al*. USP18 recruits USP20 to promote innate antiviral response through deubiquitinating STING/MITA. Cell Res. 2016;26(12): 1302-19.
17. Arimoto KI, Miyauchi S, Troutman TD, Zhang Y, Liu M, Stoner SA, *et al*. Expansion of interferon inducible gene pool via USP18 inhibition promotes cancer cell pyroptosis. Nat Commun. 2023; 14(1):251.
18. Hou J, Han L, Zhao Z, Liu H, Zhang L, Ma C, *et al*. USP18 positively regulates innate antiviral immunity by promoting K63-linked polyubiquitination of MAVS. Nat Commun. 2021;12(1):2970.
19. Ying X, Zhao Y, Yao T, Yuan A, Xu L, Gao L, *et al*. Novel protective role for ubiquitin-specific protease 18 in pathological cardiac remodeling. hypertension. 2016;68(5):1160-70.
20. Wu QQ, Liu C, Cai Z, Xie Q, Hu T, Duan M, *et al*. High-mobility group AT-hook 1 promotes cardiac dysfunction in diabetic cardiomyopathy via autophagy inhibition. Cell Death Dis. 2020;11(3):160.
21. Liu C, Hu T, Cai Z, Xie Q, Yuan Y, Li N, *et al*. Nucleotide-binding oligomerization domain-like receptor 3 deficiency attenuated isoproterenol-induced cardiac fibrosis via reactive oxygen species/high mobility group box 1 protein axis. Front Cell Dev Biol. 2020;8:713.
22. Nunes JPS, Andrieux P, Brochet P, Almeida RR, Kitano E, Honda AK, *et al*. Co-exposure of cardiomyocytes to IFN-γ and TNF-α induces mitochondrial dysfunction and nitro-oxidative stress: implications for the pathogenesis of chronic chagas disease cardiomyopathy. Front Immunol. 2021;12:755862.
23. Liu W, Deng J, Xu J, Wang H, Yuan M, Liu N, *et al*. High-mobility group box 1 (HMGB1) downregulates cardiac transient outward potassium current (Ito) through downregulation of Kv4.2 and Kv4.3 channel transcripts and proteins. J Mol Cell Cardiol. 2010;49(3):438-48.
24. Wu QQ, Yao Q, Hu TT, Wan Y, Xie QW, Zhao JH, *et al*. Tax1 banding protein 1 exacerbates heart failure in mice by activating ITCH-P73-BNIP3-mediated cardiomyocyte apoptosis. Acta Pharmacol Sin. 2022;43(10):2562-72.
25. Gomez D, Baylis RA, Durgin BG, Newman AAC, Alencar GF, Mahan S, *et al*. Interleukin-1β has atheroprotective effects in advanced atherosclerotic lesions of mice. Nat Med. 2018;24(9):1418-29.
26. Kang JA, Jeon YJ. Emerging roles of USP18: from biology to pathophysiology. Int J Mol Sci. 2020;21(18):6825.
27. Ashrafi G, Schwarz TL. The pathways of mitophagy for quality control and clearance of mitochondria. Cell Death Differ. 2013; 20(1):31-42.
28. Mizumura K, Cloonan SM, Nakahira K, Bhashyam AR, Cervo M, Kitada T, *et al*. Mitophagy-dependent necroptosis contributes to the pathogenesis of COPD. J Clin Invest. 2014;124(9):3987-4003.
29. Mustachio LM, Kawakami M, Lu Y, Rodriguez-Canales J, Mino B, Behrens C, *et al*. The ISG15-specific protease USP18 regulates stability of PTEN. Oncotarget. 2017;8(1):3-14.
30. Shiba-Fukushima K, Arano T, Matsumoto G, Inoshita T, Yoshida S, Ishihama Y, *et al*. Phosphorylation of mitochondrial polyubiquitin by PINK1 promotes Parkin mitochondrial tethering. PLoS Genet. 2014;10(12):e1004861.
31. Ketscher L, Hannss R, Morales DJ, Basters A, Guerra S, Goldmann T, *et al*. Selective inactivation of USP18 isopeptidase activity *in vivo* enhances ISG15 conjugation and viral resistance. Proc Natl Acad Sci U S A. 2015;112(5):1577-82.
32. Hopkins BD, Fine B, Steinbach N, Dendy M, Rapp Z, Shaw J, *et al*. A secreted PTEN phosphatase that enters cells to alter signaling and survival. Science. 2013;341(6144):399-402.
33. Dziamałek-Macioszczyk P, Harazny JM, Kwella N, Wojtacha P, Jung S, Dienemann T, *et al*. Relationship between ubiquitin-specific peptidase 18 and hypertension in Polish adult male subjects: a cross-sectional pilot study. Med Sci Monit. 2020;26:e921919.
34. Wang S, Long H, Hou L, Feng B, Ma Z, Wu Y, *et al*. The mitophagy pathway and its implications in human diseases. Signal Transduct Target Ther. 2023;8(1):304.
35. Forte M, D'Ambrosio L, Schiattarella GG, Salerno N, Perrone MA, Loffredo FS, *et al*. Mitophagy modulation for the treatment of cardiovascular diseases. Eur J Clin Invest. 2024;54(8):e14199.
36. Rabinovich-Nikitin I, Rasouli M, Reitz CJ, Posen I, Margulets V, Dhingra R, *et al*. Mitochondrial autophagy and cell survival is regulated by the circadian Clock gene in cardiac myocytes during ischemic stress. Autophagy. 2021;17(11):3794-812.
37. Zhang H, Yang N, He H, Chai J, Cheng X, Zhao H, *et al*. The zinc transporter ZIP7 (Slc39a7) controls myocardial reperfusion injury by regulating mitophagy. Basic Res Cardiol. 2021;116(1):54.
38. Ma ZR, Xiong QW, Cai SZ, Ding LT, Yin CH, Xia HL, *et al*. USP18 enhances the resistance of BRAF-mutated melanoma cells to vemurafenib by stabilizing cGAS expression to induce cell autophagy. Int Immunopharmacol. 2023;122:110617.
39. Wang L, Lu G, Shen HM. The long and the short of PTEN in the regulation of mitophagy. Front Cell Dev Biol. 2020;8:299.
40. Degli Esposti M. Did mitophagy follow the origin of mitochondria?. Autophagy. 2024;20(5):985-93.
41. Onishi M, Yamano K, Sato M, Matsuda N, Okamoto K. Molecular mechanisms and physiological functions of mitophagy. EMBO J. 2021;40(3):e104705.
42. Cai J, Li R, Xu X, Zhang L, Lian R, Fang L, *et al*. CK1α suppresses lung tumour growth by stabilizing PTEN and inducing autophagy. Nat Cell Biol. 2018;20(4):465-78.
43. Liang H, He S, Yang J, Jia X, Wang P, Chen X, *et al*. PTENα, a PTEN isoform translated through alternative initiation, regulates

mitochondrial function and energy metabolism. Cell Metab. 2014;19(5):836-48.
44. Song X, He J, Shi B, Han Y. Hypoxic microenvironment-induced reduction in PTEN-L secretion promotes non-small cell lung cancer metastasis through PI3K/Akt pathway. Evid Based Complement Alternat Med. 2022;2022:6683104.

https://doi.org/10.1016/j.mmr.2026.100004
Cite this article as: Wu QQ, Xiao Y, Hu YY, Yang XY, Yan XY, Deng KQ, *et al*. USP18 exacerbates myocardial I/R injury by inhibiting Parkin mitophagy through the deubiquitinase PTEN-L. *Mil Med Res*. 2026;13(1):100004.